

One-dimensional quantum wires: A pedestrian approach to bosonization

Sebastian Eggert

University of Kaiserslautern

Dept. of Physics, Erwin-Schrödinger Str.

D-67663 Kaiserslautern, Germany

Contents

1	Introduction	2
1.1	What are quantum wires?	2
1.1.1	Band structure	2
1.1.2	Creating quantum wires: Experiments	4
1.1.3	Models in second quantization	6
1.2	What is measured?	9
1.2.1	Tunneling	9
1.2.2	Photoemission spectroscopy	11
1.2.3	Conductivity	12
2	Bosonic description	14
2.1	Linearization of the fermion dispersion	14
2.2	Excitation spectrum	17
2.3	Bosonic operators	19
2.4	Fermion operators in terms of bosons	22
2.4.1	Left- and right-moving fermion densities	23
2.4.2	Boson field operator	25
2.4.3	Fermion field	26
2.4.4	Field commutators	28
2.4.5	Bosonic excitation and zero modes	30
2.4.6	Summary of the bosonization formulas	31
2.5	Correlation functions	32
2.5.1	In space	32
2.5.2	In time	34
2.6	Spin-charge separation	35

2.6.1	Spin and charge excitations	35
2.6.2	Spin and charge correlation functions	37
3	Electron-electron interactions	38
3.1	Scattering processes	38
3.2	The Luttinger Liquid parameter: Boguliov transformation	40
3.3	Correlation functions	42
4	Appendix: The boson cummulant formula	44

1 Introduction

In these lecture notes we will consider systems in which the motion of electrons is confined to one dimension (1D). In these so-called *quantum wires* electron-electron interaction effects play an important role because the restricted dimensions enhance the scattering between the electrons and completely destroy the quasi-particle picture. New density wave excitations appear that are described by bosonic operators. Here we will develop this bosonic description, following a “pedestrian” approach which does not require any previous knowledge in field theory methods. These notes therefore serve as a detailed introduction into bosonization by carefully deriving the most fundamental formulas. For advanced topics we recommend to consult one of the more sophisticated reviews on bosonization [1–5] for further reading.

1.1 What are quantum wires?

Before we address many-body effects, let us review some introductory material in order to define what quantum wires are, what can be measured in typical experimental setups and what theoretical models we wish consider.

1.1.1 Band structure

In the classical world we have some intuition on how to create a one-dimensional transport channel for particles. In order to make it truly one-dimensional we could simply narrow a pipe until two particles can no longer pass each other, for example by creating a narrow path for pedestrians until they can only walk in single file. It is easy to imagine how a stop-and-go density wave will be created in such a situation. In quantum physics, particles are instead described by wave-functions, which are known to be given by discrete standing waves when we confine an electron with box-like boundary conditions as for example shown in Fig. 1 for a simplified square wire. The allowed standing waves must have wave-numbers that fit in the square potential along the x - and y -directions, i.e. $d = n_x \frac{\lambda_x}{2} = n_x \frac{\pi}{k_x}$ and $d = n_y \frac{\lambda_y}{2} = n_y \frac{\pi}{k_y}$

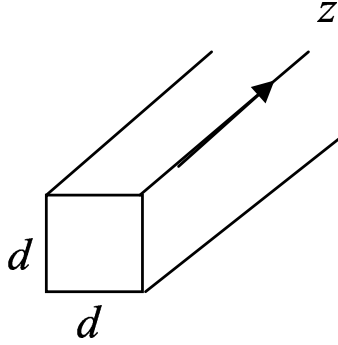


Figure 1: Confinement in a square wire

while the motion in the z -direction is unrestricted. The allowed k -vectors are therefore along quantization lines which cut the band-structure of the material of the wire. This situation is depicted in Fig. 2, where only the x - and z -direction is shown. The original Fermi surface of the material of the wire is schematically drawn dotted in this plane. Small energy excitations are now only possible along the quantization lines and close to the Fermi surface. Each quantization line that crosses the Fermi surface therefore corresponds to a “channel”, which contributes to the conductivity with quantized conductance as we will see later.

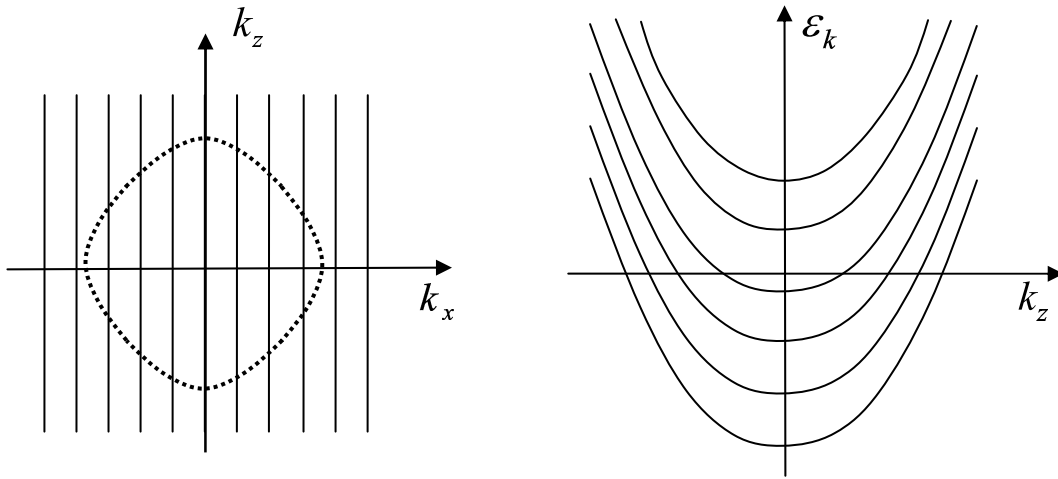


Figure 2: Cross section of Fermi surface. Vertical lines are the 1D quantization lines. Right: Effective one-dimensional band-structure along the z -direction.

For a truly one-dimensional wire we would like to have only one single channel that crosses the Fermi surface, i.e. only two Fermi points corresponding to left- and right-moving electrons. For this to be true, the energy spacing between the quantization lines must be larger than the depth of the Fermi-surface as shown in Fig. 3. For an order-of-magnitude estimate of

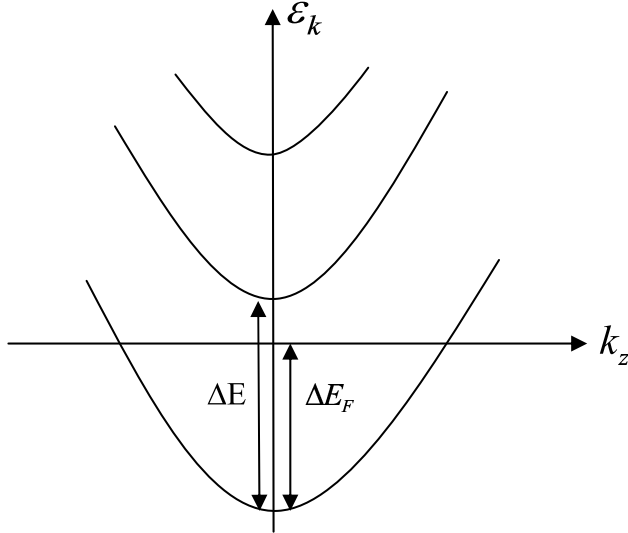


Figure 3: Electron bands where the energy spacing is larger than the depth of Fermi sea.

the required length scale of d we can assume that the bandwidth is about a few eV and the dispersion is given by an effective mass $E = \hbar^2 k^2 / 2m^*$. Together with $k = n\pi/d$ the condition $\Delta E > \Delta E_F$ gives $\Delta E = \frac{\hbar^2}{2m^*} \left(\frac{\pi}{d}\right)^2 \gtrsim 1\text{eV}$. Using $1Ry = \frac{\hbar^2}{2ma_0^2} \approx 13.6\text{eV}$ and $a_0 \approx 0.5\text{\AA}$, we finally arrive at the estimate:

$$d < \pi \sqrt{\frac{\hbar^2}{2m^* \text{eV}}} = \pi \sqrt{\frac{a_0^2 Ry}{\text{eV}}} = \pi \sqrt{13.6} a_0 \approx 0.5\text{nm}$$

We therefore find that diameters of one nanometer or less are required in order to observe one-dimensional physics. For semi-conductors the bandwidth and the effective mass can be much smaller, so that a few nanometers may be possible. For metallic wires, however, essentially single atomic chains are required.

1.1.2 Creating quantum wires: Experiments

The creation of one dimensional wires is therefore still a great challenge even with today's semiconductor technology, which can create structures that are only a few tens of nanometers in size. However, even if traditional processing techniques of lithography and etching can be scaled down to about 10nm, the resulting structures are still imprecise on a nanometer scale. The resulting wire typically has relatively uncontrolled wavy edges, which immediately leads to localization in a one-dimensional system. In order to produce a wire that has perfect translational invariance, we therefore require production mechanisms that give full control down to the atomic scale. We will briefly describe three of the most promising experimental

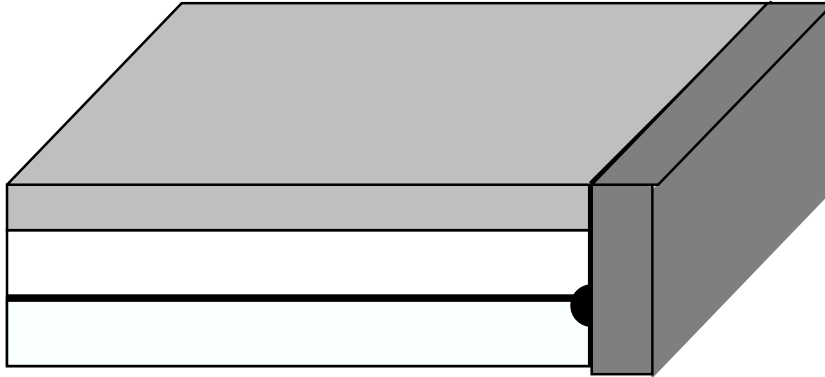


Figure 4: 1D wire created by cleaved edge overgrowth. [6]

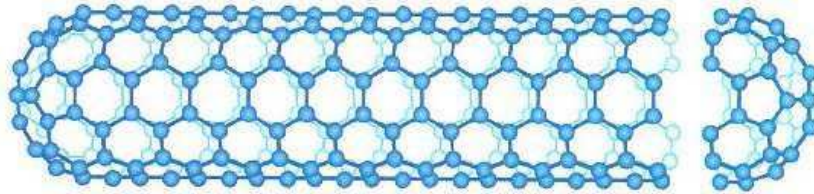


Figure 5: A carbon nanotube.

approaches below.

Using molecular beam epitaxy it is possible to grow atomically perfect structures layer by layer. In this way it is now standard to create high quality two-dimensional electron gas (2DEG) systems by use of an inversion layer. In the so-called cleaved edge overgrowth technique such a sample is then cleaved in-situ [6]. The cleaved edge is typically along one of the crystal axis and also atomically perfect. If a gate is overgrown on the edge, it is then possible to apply a suitable potential that forces the mobile electrons to be trapped in the one dimensional wire that is defined by the intersection of the 2DEG and the cleaved edge as shown in Fig. 4. A suppression of the density of states which is consistent with the theory has been demonstrated in such a setup [7].

Another approach to create atomically perfect structures is to use macromolecules that form a tubular structure. The most famous examples are the carbon nanotubes as shown in Fig. 5. Even though the detailed diameter and location of the tubes cannot be fully controlled in the production process, the chemical composition guarantees that the resulting tubes are atomically perfect structures on the nanoscale. Several experiments showed that single wall carbon nanotubes exhibit the signatures of a one-dimensional many-body system [8–10] consistent with theory [11–13].

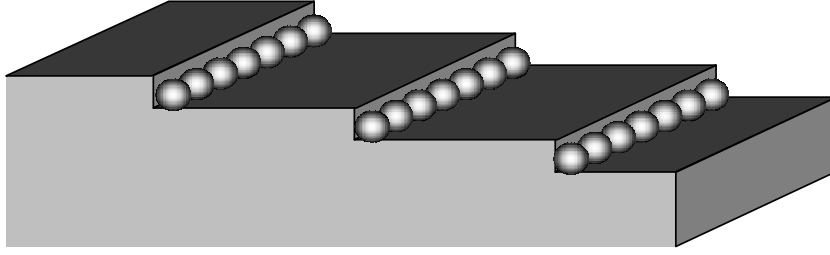


Figure 6: Atomic Au chains deposited on Si step edges. [14]

Superstructures on extremely clean surfaces, like a stepped silicon surface are a third example [14]. Cleaving a Si(111) surface at a slight angle creates a regular step structure on which small amounts of gold can be deposited. The gold atoms tend to form atomic chains along the steps of the silicon, a so-called Si(111) 5x1 Au structure as shown in Fig. 6. Experiments were able to find the signature of spin-charge separation using photoemission on such samples [14].

Other possible experimental realizations of one-dimensional wires include quantum hall edges, stretched point contacts, and intrinsically quasi-low dimensional compounds.

1.1.3 Models in second quantization

Let us now define the basic theoretical models for quantum wires. The Hamiltonian for an arbitrary band-structure of non-interacting fermions as shown in Fig. 7 can always be written in the formalism of second quantization

$$H = \sum_{k,\sigma} \varepsilon_k c_{k,\sigma}^\dagger c_{k,\sigma} \quad (1)$$

Here the operator $c_{k,\sigma}^\dagger$ creates a single electron $|k,\sigma\rangle = c_{k,\sigma}^\dagger |0\rangle$ in a Bloch eigenstate of the system and the annihilation operator $c_{k,\sigma}$ annihilates a particle. These operators are defined for each spin index $\sigma = \uparrow, \downarrow$ and each band separately and are summed over independently in the Hamiltonian. Spin and band indices will be suppressed in what follows until section 2.6. For simplicity we can assume periodic Born-von Karman boundary conditions over a finite length $\ell = Na$, which leads to discrete k values of $k = 2\pi n/N$. The usual anti-commutation relations for fermion operators must be obeyed

$$\begin{aligned} \{c_k^\dagger, c_k\} &= c_k^\dagger c_k + c_k c_k^\dagger = \delta_{k,k'} \\ \{c_k^\dagger, c_k^\dagger\} &= 0 = \{c_k c_k\} \end{aligned} \quad (2)$$

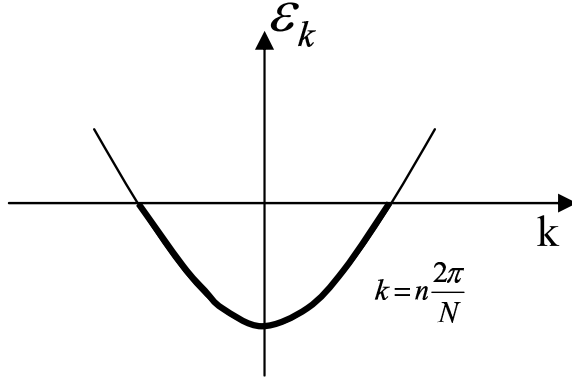


Figure 7: Non-interacting electron dispersion.

This ensures that the wave-function that is created by these operators is automatically anti-symmetric under particle exchange. Also the Pauli Exclusion Principle of no double occupancy $c_k^\dagger c_k^\dagger = 0$ is obeyed. The number operator $n_k = c_k^\dagger c_k$ in the Hamiltonian counts the number of fermions in the state $|k\rangle$ with eigenvalues of 0 and 1, i.e.

$$c_k^\dagger c_k |0\rangle = 0 \quad (3)$$

and

$$c_k^\dagger c_k |k\rangle = c_k^\dagger c_k c_k^\dagger |0\rangle = \left(c_k^\dagger \{c_k, c_k^\dagger\} - c_k^\dagger c_k^\dagger c_k \right) |0\rangle = c_k^\dagger |0\rangle = |k\rangle \quad (4)$$

The Fourier transforms of the Bloch operators correspond to field operators

$$\psi(x_j) = \frac{1}{\sqrt{N}} \sum_{k=-\pi}^{\pi} e^{ikj} c_k, \quad (5)$$

which also obey canonical anti-commutation relations. Here $x_j = ja$ with $j = 1, \dots, N$ labels the locations in the one-dimensional lattice with lattice spacing a . Therefore, $\psi^\dagger(x_j)$ creates an electron in a localized Wannier state at lattice site x_j . The field operator is periodic $\psi(x_j) = \psi(x_{j+N})$ since $e^{ikN} = 1$ for $k = 2\pi n/N$. The inverse Fourier transform is given by

$$c_k = \frac{1}{\sqrt{N}} \sum_{j=1}^N e^{-ikj} \psi(x_j). \quad (6)$$

Example: Tight binding model

In order to illustrate the use of second quantization in a simple model, we consider hopping

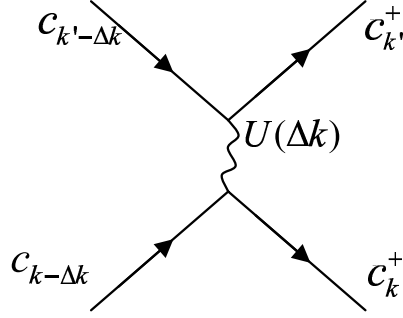


Figure 8: The interaction corresponds to a scattering process.

between neighboring orbitals along a chain. The field operator $\psi(x_j)$ now creates an electron in the orbital wave-function $\phi(\vec{r} - \vec{r}_j)$, where \vec{r}_j is the three dimensional coordinate of the lattice site x_j . The so-called tight binding Hamiltonian is represented by overlap integrals $t = -\int d^3\vec{r} \phi(\vec{r}_j) \Delta H \phi^*(\vec{r}_{j+1})$ between neighboring orbitals, which allows transitions of the electrons (“hopping”). In second quantization this Hamiltonian is given by

$$H = -t \sum_j \left(\psi^\dagger(x_j) \psi(x_{j+1}) + \psi^\dagger(x_{j+1}) \psi(x_j) \right) \quad (7)$$

Using the Fourier transform (5), we get

$$\begin{aligned} H &= -\frac{t}{N} \sum_j \sum_k \sum_{k'} \left(e^{-ikj} c_k^\dagger e^{ik'(j+1)} c_{k'} + e^{-ik'(j+1)} c_{k'}^\dagger e^{ikj} c_k \right) \\ &= -t \sum_k \left(e^{ik} c_k^\dagger c_k + e^{-ik} c_k^\dagger c_k \right) \\ &= -2t \sum_k n_k \cos k \end{aligned} \quad (8)$$

where we have used the identity $\sum_{j=1}^N e^{ikj} = N\delta_k$ which follows from the geometrical sum

$\sum_{j=0}^N q^j = \frac{1-q^{N+1}}{1-q}$. This is an illustration of a band structure $\varepsilon_k = -2t \cos k$ with cosine dependence where $n_k = c_k^\dagger c_k$ counts number of fermions in the state k .

Interactions

The understanding of electron-electron interaction effects is the main motivation for bosonization. The standard model of a generic density-density interaction is represented by a two particle operator. If the interaction potential between electrons in Wannier states at distance

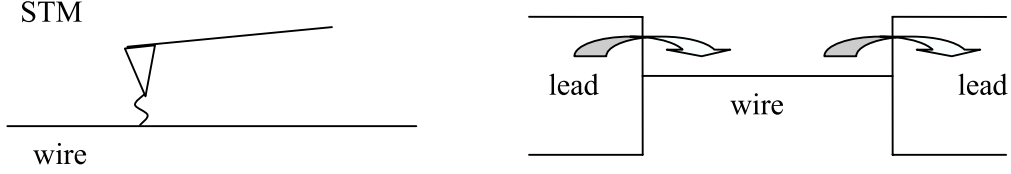


Figure 9: Two tunneling examples: scanning tunneling microscopy and a conducting wire between two electrodes

m is given by $U(m)$, the corresponding interaction Hamiltonian can be expressed in second quantization using the fermion density operator $\rho(x_j) = \psi^\dagger(x_j)\psi(x_j)$ as

$$\begin{aligned}
 H_{\text{int}} &= \sum_{j=1}^N \sum_{m=1}^N \psi^\dagger(x_j)\psi(x_j)U(m)\psi^\dagger(x_{j+m})\psi(x_{j+m}) \\
 &= \frac{1}{N^2} \sum_{j=1}^N \sum_{m=1}^N \sum_{k,k'} c_k^\dagger c_{k'} e^{-ikj} e^{ik'j} U(m) \sum_{k'',k'''} c_{k''}^\dagger c_{k'''} e^{-ik''(j+m)} e^{ik'''(j+m)} \quad (9)
 \end{aligned}$$

The sum over j results in a delta function with the condition $k - k' = k''' - k'' = \Delta k$, so that,

$$\begin{aligned}
 H_{\text{int}} &= \frac{1}{N} \sum_{m=1}^N \sum_{k,k'',\Delta k} c_k^\dagger c_{k-\Delta k} U(m) c_{k''}^\dagger c_{k''+\Delta k} e^{i\Delta k m} \\
 &= \frac{1}{N} \sum_{k,k'',\Delta k} c_k^\dagger c_{k-\Delta k} U(\Delta k) c_{k''}^\dagger c_{k''+\Delta k} \quad (10)
 \end{aligned}$$

where we have used the Fourier transform and defined $U(\Delta k) = \sum_m e^{i\Delta k m} U(m)$. The two particle interaction therefore corresponds to a scattering process as represented in the diagram in Fig. 8. Particles $c_{k'-\Delta k}$ and $c_{k-\Delta k}$ are annihilated and after exchanging Δk two new particles $c_{k'}^\dagger$ and c_k^\dagger are created.

1.2 What is measured?

1.2.1 Tunneling

Tunneling is a common experimental setup for quantum wires. One example is scanning tunneling microscopy (STM), where tunneling occurs across the gap between the wire and the STM tip. A second example would be a 1D wire, that is weakly connected to two leads at the ends, where tunneling may occur. In those experiments the current is determined by the

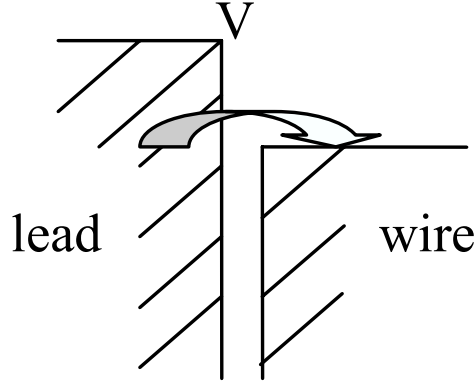


Figure 10: Schematic diagram of tunneling from a lead/tip to a wire

tunneling rate, which is given by Fermi's Golden Rule

$$\Gamma^+(\omega, x) = \frac{2\pi t^2}{Z} \sum_{n,m} e^{-\beta E_m} \left| \langle n | \psi^\dagger(x) | m \rangle \right|^2 \delta(\omega - E_n + E_m). \quad (11)$$

Here the probability of the transition from state $|m\rangle$ to $|n\rangle$ by adding one particle is considered. The tunneling Hamiltonian between the lead/tip and the wire is assumed to be $H = -t(\psi^\dagger(x)\psi_{leads} + h.c.)$ and Z is the partition function. The tunneling current can be calculated from the tunneling rates by considering the empty and occupied states relative to the Fermi level given by the Fermi-Dirac distribution, $f(\omega) = 1/(1 + e^{\beta\omega})$

$$I(V, x, \beta) = e \int_{-\infty}^{\infty} d\omega \rho_{leads}(\omega - eV) [f(\omega - eV)\Gamma^+(\omega) - (1 - f(\omega - eV))\Gamma^-(\omega)] \quad (12)$$

(Tunneling in) - (Tunneling out)

as illustrated in diagram 10. It is useful to express the tunneling rate in terms of the so-called *local spectral weight*, defined as

$$A(\omega, x, \beta) = \frac{1 + e^{-\beta\omega}}{Z} \sum_{n,m} e^{-\beta E_m} \left| \langle n | \psi^\dagger(x) | m \rangle \right|^2 \delta(\omega - E_n + E_m) = \frac{1 + e^{-\beta\omega}}{2\pi t^2} \Gamma^+, \quad (13)$$

assuming finite temperatures $\beta = 1/k_B T$. Inserting (13) into the expression for the current (12) and performing straightforward calculations using the Fermi-Dirac distribution, we arrive at a simple equation for $I(V, x)$ in terms of the local spectral weight

$$I(V, x, \beta) = 2\pi t^2 e \int_{-\infty}^{\infty} d\omega \rho_{leads}(\omega - eV) (f(\omega - eV) - f(\omega)) A(\omega, x). \quad (14)$$

Finally, in order to calculate the local spectral weight $A(\omega, x)$, we can rewrite the delta function as $\delta(\omega) = \frac{1}{2\pi} \int_{-\infty}^{+\infty} e^{i\omega t} dt = \text{Re} \frac{1}{\pi} \int_0^{\infty} e^{i\omega t} dt$, so that from (13)

$$A(\omega, x) = \frac{1}{Z} \sum_{n,m} (e^{-\beta E_n} + e^{-\beta E_m}) \left| \langle n | \psi^\dagger(x) | m \rangle \right|^2 \text{Re} \frac{1}{\pi} \int_0^{\infty} e^{i(\omega - E_n + E_m)t} dt \quad (15)$$

Then, using $e^{iHt} |m\rangle = e^{iE_m t} |m\rangle$, we arrive at the Green's function representation

$$\begin{aligned} A(\omega, x) &= \text{Re} \left(\frac{1}{\pi Z} \sum_{n,m} \int_0^{\infty} dt e^{i\omega t} (e^{-\beta E_m} + e^{-\beta E_n}) \langle n | \psi^\dagger | m \rangle \langle m | e^{iHt} \psi e^{-iHt} | n \rangle \right) \\ &= \text{Re} \frac{1}{\pi} \int_0^{\infty} dt e^{i\omega t} \langle \psi(x, t) \psi^\dagger(x, 0) + \psi^\dagger(x, 0) \psi(x, t) \rangle \\ &= \frac{1}{\pi} \text{Im} \int_0^{\infty} G^R(t, x) e^{i\omega t} dt \end{aligned} \quad (16)$$

where $G^R(t, x)$ is the retarded Green's function

$$G^R(t, x) = -i \langle \{ \psi(x, t), \psi^\dagger(x, 0) \} \rangle \theta(t). \quad (17)$$

Here the thermal expectation value $\langle A \rangle = \sum_n e^{-\beta E_n} \langle n | A | n \rangle / Z$ is used. At zero temperature the local spectral weight reduces to the *local density of states* (LDOS)

$$\rho(\omega, x) = \sum_m \left| \langle m | \psi^\dagger(x) | 0 \rangle \right|^2 \delta(\omega - \epsilon_m) = \frac{1}{\pi} \text{Im} \int_0^{\infty} G^R(t, x) e^{i\omega t} dt \quad (18)$$

and the current is

$$I(V, x, \beta) = 2\pi t^2 e \int_0^{eV} d\omega \rho_{leads}(\omega - eV) \rho(\omega, x) \quad (19)$$

Since Green's functions such as (17) play a central role in condensed matter physics, it will be one of the main goals in the many-body theory to calculate time correlation functions.

1.2.2 Photoemission spectroscopy

Photoemission spectroscopy (PES) is a standard technique to determine the electronic properties of condensed matter systems. Photons with definite energy and direction strike an object and electrons are emitted via the photoelectric effect as shown in Fig. 11. In return, the intensity of the electrons as a function of absorbed energy and momentum gives information about the object. In inverse photoemission electrons are used to probe the sample and the emitted photons are analyzed correspondingly. Interestingly the mathematical description is very similar to the tunneling processes considered above. Just as before, we can argue that

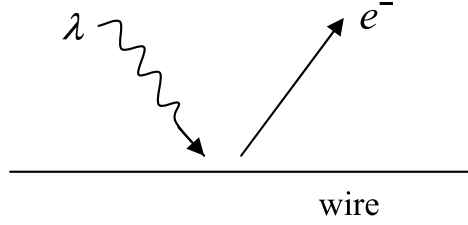


Figure 11: Schematic diagram of photoemission

the emission rate of photons Γ^+ in inverse photoemission at a given energy and wave-vector is related to the probability for adding a corresponding electron into the system. According to Fermi's Golden Rule

$$\Gamma^+(\omega, q, \beta) \propto \frac{1}{Z} \sum_{n,m} e^{-\beta E_m} |\langle n | c_q^\dagger | m \rangle|^2 \delta(\omega - E_n + E_m), \quad (20)$$

where now the probability of the transition from state $|m\rangle$ to $|n\rangle$ by adding one particle with wave-vector q is the relevant quantity. In this case it is useful to define the *angle resolved spectral density*

$$A(\omega, q, \beta) = \frac{1 + e^{-\beta\omega}}{Z} \sum_{n,m} e^{-\beta E_m} \left| \langle n | c_q^\dagger | m \rangle \right|^2 \delta(\omega - E_n + E_m) \propto \Gamma^+(\omega, q). \quad (21)$$

The angle integrated spectral density and the space integrated local spectral weight in equation (13) are always the same and represent the total spectral weight as a function of ω . Following the analogous calculations as in the previous section we can calculate the angle resolved spectral density in terms of a retarded Green's function in momentum space

$$A(\omega, q, \beta) = -\frac{1}{\pi} \text{Im} \int_0^\infty dt e^{i\omega t} G^R(t, q, \beta), \quad (22)$$

where

$$G^R(t, q, \beta) = -i \left\langle \left\{ c_q(t), c_q^\dagger(0) \right\} \right\rangle. \quad (23)$$

1.2.3 Conductivity

When speaking about the physics of “wires”, it is natural to think about the corresponding conductivity. However, in order to apply a voltage and measure the current, perfect contacts to external leads are required, which cannot be realized in most experiments with truly one-dimensional wires. Nonetheless, let us imagine a setup in which electrons are adiabatically guided into a single-channel wire of length ℓ without any scattering under an applied voltage

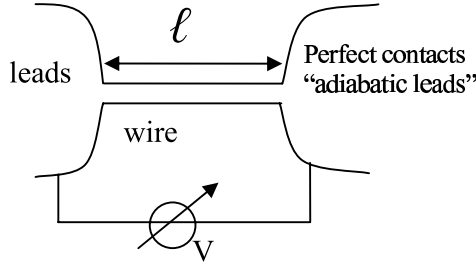


Figure 12: Schematic diagram of metallic leads and a 1D wire

V as shown in Fig. 12.

The standard theory of linear response gives the general conductivity in terms of the Kubo formula

$$\sigma(q, \omega) = \frac{1}{\omega} \int_0^\infty e^{i\omega t} \langle [J(q, t), J(-q, t)] \rangle. \quad (24)$$

Naively the DC conductivity is then simply given by $\sigma(0, 0)$, but since we are dealing with a finite wire it turns out that it makes a difference if we first take the limit $\omega \rightarrow 0$ (current oscillating between the leads) or the limit $q \rightarrow 0$ (current oscillating within the wire). In the latter case we obtain

$$G(\omega) = \lim_{q \rightarrow 0} \sigma(q, \omega) = \frac{1}{\ell \omega} \int_0^\ell dx \int_0^\infty dt e^{i\omega t} \langle [J(x, t), J(0, 0)] \rangle. \quad (25)$$

For interacting systems the outcome actually depends on the order of limits. However, we will not address this question here. Instead we consider a perfect ballistic non-interacting wire in order to show that even in this simplest case the conductivity is finite and quantized. In fact, we can derive the conductivity without the calculation of correlation functions by considering the semi-classical acceleration of electrons in the field of an applied voltage $E = V/\ell$. The crystal momentum changes with the applied force $\hbar \dot{k} = -F = eE = eV/\ell$. The current is given by the number of electrons in current carrying states per unit time. The number of electrons that contribute to the current is simply given by counting the states in an interval Δk as # of $e^- = \Delta k \ell / 2\pi$ (see Fig. 13). Since electrons are constantly ejected into the right lead, the number of electrons in the current carrying states remains finite and can be determined by the number of electrons that are accelerated into those states per unit time via the following simple calculation

$$I = e \frac{\# \text{ of } e^-}{\Delta t} = e \frac{\Delta k}{\Delta t} \frac{\ell}{2\pi} = e \dot{k} \frac{\ell}{2\pi} = \frac{e^2 V}{2\pi \hbar} = GV$$

where $G = e^2/h$ is the quantized conductance per ballistic channel ($2e^2/h$ for electrons with

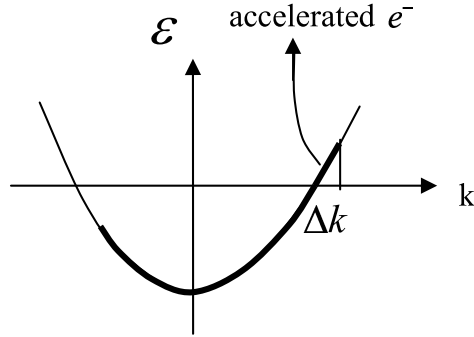


Figure 13: Electrons are accelerated by the voltage into current carrying states.

spin). The corresponding energy is dissipated in the right lead where the accelerated electrons quickly reach thermal equilibrium, while the wire remains cold. In general it is also possible to take a finite transmission and several channels into account, which gives

$$G = \sum_{\text{channels } n} t_n \frac{2e^2}{h}$$

where $0 < t_n \leq 1$ are the eigenvalues of the transmission matrix $T^\dagger T$ between the n different channels. This is the famous Landauer-Büttiker formula for quantized conductance of wires and point contacts.

2 Bosonic description

2.1 Linearization of the fermion dispersion

A bosonic description of the one-dimensional wire will be useful in the treatment of interactions. Let us first show in detail how a non-interacting fermionic system given in equation (1) can be expressed in terms of a bosonic Hamiltonian in second quantization. For this equivalence to work we require the dispersion relation of the fermions to be linear in the range of interest. This is always approximately true for excitations with small energy around the Fermi points. Therefore, we will restrict ourselves to consider low enough energies so that we can describe the band structure in equation (1) by an energy that depends linearly on the wave vector k , which is the only approximation we will make. The starting point is an arbitrary free electron dispersion in equation (1)

$$H = \sum_{k,\sigma} \varepsilon_k c_{k,\sigma}^\dagger c_{k,\sigma} \quad (26)$$

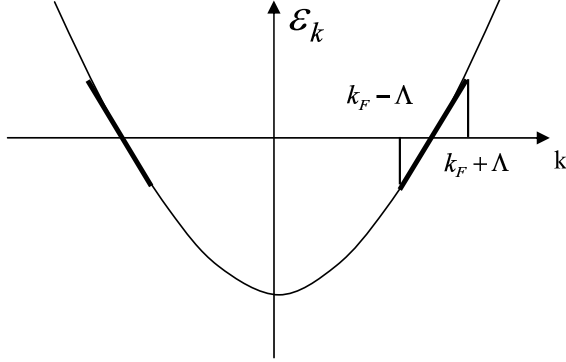


Figure 14: Allowed k -values around $\pm k_F$

At zero temperature all states between the Fermi wave-vectors $-k_F$ to k_F are occupied. The number of particles in the Fermi sea is therefore given by

$$n_0 = k_F N / \pi - 1 \quad (27)$$

if n_0 is even, or $n_0 = k_F N / \pi$ if n_0 is odd (times two for electrons with spin).

Since we are only interested in low energy excitations, we now restrict the allowed wave-numbers to a range Λ around the Fermi points $-k_F - \Lambda < k < -k_F + \Lambda$ and $k_F - \Lambda < k < k_F + \Lambda$ as shown in Fig. 14 corresponding to right- (k_F) and left-moving ($-k_F$) fermions, respectively. The range Λ is determined by the region over which the band structure is approximately linear and depends on the model (typically corresponding to an energy range of about 1/10 of the band width). Keeping only states in this range the *linearized effective Hamiltonian* is given by

$$H \approx \sum_{k=k_F-\Lambda}^{k_F+\Lambda} \varepsilon_k c_k^\dagger c_k + \sum_{k=-k_F-\Lambda}^{-k_F+\Lambda} \varepsilon_k c_k^\dagger c_k \quad (28)$$

In this range the energy dispersion can be expanded around $\pm k_F$

$$\varepsilon_k \approx \varepsilon_{k_F} + (k - k_F) \left. \frac{\partial \varepsilon_k}{\partial k} \right|_{k_F} + O \left[(k - k_F)^2 \right] \quad \text{for } k \approx k_F \quad (29)$$

for the “right movers” and analogously

$$\varepsilon_k \approx \varepsilon_{-k_F} + (k + k_F) \left. \frac{\partial \varepsilon_k}{\partial k} \right|_{-k_F} + O \left[(k + k_F)^2 \right] \quad \text{for } k \approx -k_F \quad (30)$$

for the “left movers”. Here the Fermi energy $\varepsilon_{-k_F} = \varepsilon_{k_F} = 0$ must be zero since all occupied states have negative energy and all empty states have positive energy at zero temperature.

Defining a Fermi velocity

$$v_F = \left. \frac{\partial \varepsilon_k}{\partial k} \right|_{k_F} = - \left. \frac{\partial \varepsilon_k}{\partial k} \right|_{-k_F} \quad (31)$$

we can therefore write $\varepsilon_k \approx v_F(k - k_F)$ for right movers and $\varepsilon_k \approx -v_F(k + k_F)$ for left movers. It is useful to define new quantum numbers $|k| < \Lambda$ shifted relative to the Fermi points $\pm k_F$ and corresponding *left and right moving fermion operators*

$$\begin{aligned} c_k^R &= c_{k_F+k} \\ c_k^L &= c_{-k_F+k} \end{aligned} \quad (32)$$

In this way the effective Hamiltonian has the simple form

$$H \approx \sum_{k=-\Lambda}^{\Lambda} v_F k \left(c_k^{R\dagger} c_k^R - c_k^{L\dagger} c_k^L \right) \quad (33)$$

Accordingly, the original fermion field operator in equation also splits into a left and a right-moving part

$$\begin{aligned} \psi(x_j) &\approx \frac{1}{\sqrt{N}} \sum_k e^{ikj} c_k \\ &= \frac{1}{\sqrt{N}} \left(\sum_{k=k_F-\Lambda}^{k_F+\Lambda} e^{ikj} c_k + \sum_{k=\Lambda-k_F}^{-k_F-\Lambda} e^{ikj} c_k \right) \\ &= \frac{1}{\sqrt{N}} \sum_k \left(e^{ik_F j} e^{ikj} c_k^R + e^{-ik_F j} e^{ikj} c_k^L \right) \\ &= \sqrt{a} \left(e^{ik_F x_j/a} \psi_R(x_j) + e^{-ik_F x_j/a} \psi_L(x_j) \right) \end{aligned} \quad (34)$$

where we have defined left and right moving fermion fields on the length of the wire $\ell = Na$

$$\begin{aligned} \psi_R(x_j) &= \frac{1}{\sqrt{\ell}} \sum_{k=-\infty}^{\infty} c_k^R e^{ikx_j/a} \\ \psi_L(x_j) &= \frac{1}{\sqrt{\ell}} \sum_{k=-\infty}^{\infty} c_k^L e^{ikx_j/a} \end{aligned} \quad (35)$$

In those definitions it is useful to extend the range of summation to infinity, because in this way an *inverse* Fourier transform can be defined as a continuous integral

$$c_k^{L/R} = \frac{1}{\sqrt{\ell}} \int_0^\ell e^{-ikx/a} \psi_{L/R}(x) dx \quad (36)$$

One may object that we have now changed the range of summation to infinity in equations (34) and (35), since the cutoff Λ is supposed to be much smaller than the bandwidth. However, remember that Λ also represents an upper limit for the validity of the effective low energy description. Indeed, extending the states of the linear dispersion relation to infinity or leaving them out makes no difference if we always restrict ourselves to low energies, since those states will then never take part in any physical excitation. Therefore, all states with $k > \Lambda$ and $-k < -\Lambda$ are unphysical anyway. By taking the summation range to infinity we have effectively taken a continuous limit for the field operators, which is mathematically more convenient. However, this does *not* correspond to an additional approximation. Note that the anti-commutator

$$\left\{ \psi_R^\dagger(x), \psi_R(y) \right\} = \frac{1}{\ell} \sum_{kk'} e^{-ikx/a} e^{ik'y/a} \left\{ c_k^{R\dagger}, c_{k'}^R \right\} = \frac{1}{\ell} \sum_{n=-\infty}^{\infty} e^{-i2\pi n(x-y)/\ell} = \delta(x-y) \quad (37)$$

is now normalized as a delta function. In general, the normalization would actually depend on the choice of the cut-off Λ , but by including the non-physical states a more convenient field operator with canonical anti-commutation relations has been defined.

2.2 Excitation spectrum

In order to understand how the fermionic spectrum can be represented by bosons we will consider individual excited states as e.g. depicted in Fig. 15 on the right moving branch. In terms of fermionic creation and annihilation operators the state is expressed as (omitting the index R for right movers temporarily)

$$c_0^\dagger c_1^\dagger c_2^\dagger c_4^\dagger c_5^\dagger c_8^\dagger |GS\rangle, \quad (38)$$

where we use integer labeling relative to the highest occupied state of the Fermi sea for simplicity¹

$$n = kN/2\pi + 1/2. \quad (39)$$

Note that the order of the operators matters, since they anti-commute. Alternatively, we can construct this state in two parts:

1. First we create four additional fermions in the lowest unoccupied states $c_1^\dagger c_2^\dagger c_3^\dagger c_4^\dagger |GS\rangle$ as shown in Fig. 16. The energy cost for this is given by¹

$$\frac{2\pi v_F}{N} \left(\frac{1}{2} + \frac{3}{2} + \frac{5}{2} + \frac{7}{2} \right) = \frac{2\pi v_F}{N} \cdot \frac{16}{2},$$

¹Note that the Fermi level can be chosen to be in the middle between two states if n_0 is odd. The highest occupied state $n = 0$ is at $k_F - \pi/N$ and k is measured relative to k_F .

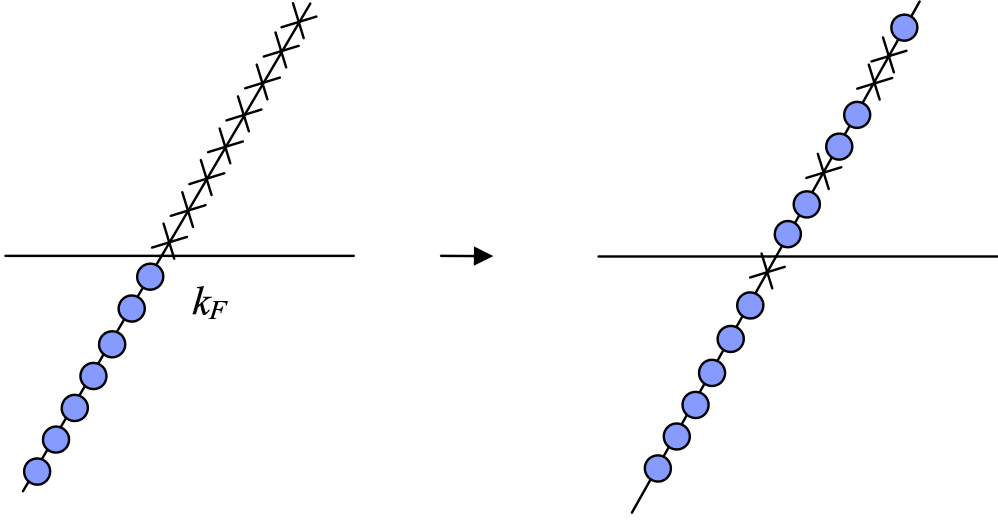


Figure 15: Left: The ground state of the filled Fermi sea $|GS\rangle$. Right: Typical excited state. The dots represent occupied states, crosses unoccupied states.

or in general by

$$E_{n_R} = \frac{\pi v_F}{N} n_R^2, \quad (40)$$

where n_R is the total number of additional right movers. The energy cost is the same for removing $-n_R$ particles.

2. Secondly we create particle-hole excitations by shifting up the individual fermions (preserving their relative order). In our case we have to

- shift the top fermion up by 4 steps with energy cost $1 \times 4 \times 2\pi v_F/N$,
- shift zero fermions by 3 steps,
- shift the two next fermions by 2 steps each with energy $2 \times 2 \times 2\pi v_F/N$
- finally shift the two next fermions up by 1 steps with energy $2 \times 1 \times 2\pi v_F/N$

By this shifting procedure any particle-hole excited state can be created. If we now interpret that each shifting by n steps corresponds to a boson of level n , the particle-hole excitations in the part 2 above would correspond to

- one excited boson on level 4, with energy $1 \times 4 \times 2\pi v_F/N$
- no bosons on level 3
- two bosons on level 2 with energy $2 \times 2 \times 2\pi v_F/N$

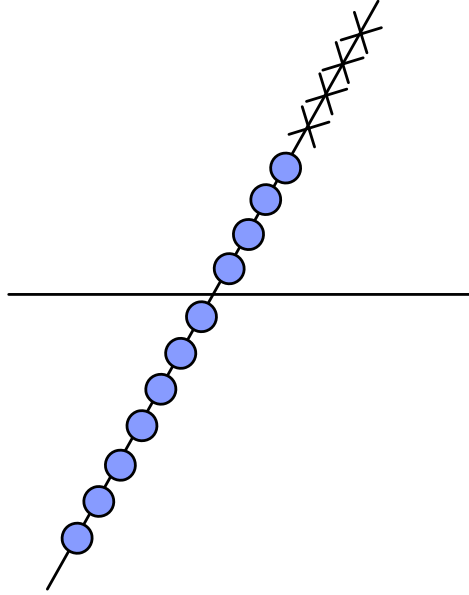


Figure 16: Excited state after adding four fermions in the lowest unoccupied levels $c_1^\dagger c_2^\dagger c_3^\dagger c_4^\dagger |GS\rangle$ after step 1.

- two bosons on level 1 with energy $2 \times 1 \times 2\pi v_F/N$

In this way any particle-hole excitation can in principle be represented by bosonic occupation numbers. This hand-waving picture is almost the entire secret to bosonization. The full story involves only a slightly more complicated linear combination of shifted states as we will see now.

2.3 Bosonic operators

From the previous section it is intuitively clear that “fermion shifting operators” may be represented by bosons. In this section we will make this mathematically precise. A good definition for a fermion shifting operator is given by

$$\rho_k^R = \sum_{k'} c_{k'+k}^{R\dagger} c_{k'}^R \quad (41)$$

This operator changes the wave-vector of right moving fermions by an amount k , summed over all possible states k' , resulting in a superposition of shifted states. This is a slight difference from the intuitive operations discussed in previous section where we have only shifted the uppermost fermions at a time (part 2), but clearly equation (41) amounts to the same basic idea.

The operator is not hermitian. In fact, the hermitian conjugate changes the k -vector by the opposite amount

$$(\rho_k^R)^\dagger = \sum_{k'=-\infty}^{+\infty} c_{k'}^{R\dagger} c_{k'+k}^R = \sum_{k'} c_{k'-k}^{R\dagger} c_{k'}^R = \rho_{-k}^R \quad (42)$$

If ρ_k^R with $k > 0$ creates an excitation as suggested in the previous section, the hermitian conjugate annihilates it, which is indeed what we would expect of bosonic operators. In the last equation we have shifted the summation variables, which is unproblematic because we have used the convenient trick of extending the summation over an infinite range as discussed above.

The final and most important step in order to relate the shifting operators in (41) to bosons are the commutation relations. Using the definition (41) we get

$$\begin{aligned} [\rho_{-k}^R, \rho_{k'}^R] &= \sum_{k'', k'''} \left(c_{k''-k}^{R\dagger} c_{k''}^R c_{k'''+k'}^{R\dagger} c_{k'''}^R - c_{k'''+k'}^{R\dagger} c_{k'''}^R c_{k''-k}^{R\dagger} c_{k''}^R \right) \\ &= \sum_{k'', k'''} \left(c_{k''-k}^{R\dagger} \left\{ c_{k''}^R, c_{k'''+k'}^{R\dagger} \right\} c_{k'''}^R - c_{k'''+k'}^{R\dagger} \left\{ c_{k''}^R, c_{k''-k}^{R\dagger} \right\} c_{k''}^R \right. \\ &\quad \left. - c_{k''-k}^{R\dagger} c_{k'''+k'}^{R\dagger} c_{k''}^R c_{k'''}^R + c_{k'''+k'}^{R\dagger} c_{k''-k}^{R\dagger} c_{k''}^R c_{k'''}^R \right) \\ &= \sum_{k''} \left(c_{k''-k}^{R\dagger} c_{k''+k'}^R - c_{k''-k+k'}^{R\dagger} c_{k''}^R \right) \\ &= 0, \end{aligned} \quad (43)$$

where the two terms on the third line cancel and we have again shifted the summation variable in the last step ($k'' \rightarrow k'' - k$). Therefore we find that the shifting operators generally commute. However, if $k = k'$, the summation variable cannot simply be shifted because in that special case the result corresponds to the subtraction of two infinities

$$[\rho_{-k}^R, \rho_k^R] = \sum_{k''} (n_{k''-k} - n_{k''}) = \infty - \infty \quad (44)$$

Indeed any arbitrary result can be produced by subtracting two infinities! However, we remember that these are not real infinities (coming from non-physical states below the lower cutoff $k < -\Lambda$). Therefore, using the fact that all states below the lower cutoff always have to be occupied, we can cancel the unphysical infinities by using the cutoff at $-\Lambda$ as a reference

point, since we require $n_k = 1$ for $k < -\Lambda$

$$\begin{aligned}
[\rho_{-k}^R, \rho_k^R] &= \sum_{k'' < -\Lambda} (n_{k''-k} - n_{k''}) + \sum_{k'' \geq -\Lambda} (n_{k''-k} - n_{k''}) \\
&= \sum_{k'' \geq -\Lambda-k} n_{k''} - \sum_{k'' \geq -\Lambda} n_{k''} \\
&= \sum_{-\Lambda > k'' \geq -\Lambda-k} n_{k''} \\
&= \frac{kN}{2\pi}
\end{aligned} \tag{45}$$

where all terms in the first sum on the first line are zero and we have used the finite level spacing $k=2\pi n/N$. In summary, we have

$$[\rho_{-k}^R, \rho_{k'}^R] = \delta_{kk'} \frac{kN}{2\pi} \tag{46}$$

which indeed corresponds to bosonic commutation relations.

For the bosonic operators to be useful we still must relate them to the Hamiltonian. Using equation (33) $H = \sum_{k'} v_F k' (c_{k'}^{R\dagger} c_{k'}^R - c_{k'}^{L\dagger} c_{k'}^L)$, the commutator with the shifting operator is given by

$$\begin{aligned}
[H, \rho_k^R] &= \sum_{k', k''} v_F k' [c_{k'}^{R\dagger} c_{k'}^R, c_{k''+k}^{R\dagger} c_{k''}^R] \\
&= \sum_{k', k''} v_F k' (c_{k'}^{R\dagger} \{c_{k'}^R, c_{k''+k}^{R\dagger}\} c_{k''}^R - c_{k''+k}^{R\dagger} \{c_{k''}^R, c_{k'}^{R\dagger}\} c_{k'}^R) \\
&= \sum_{k'} v_F k' (c_{k'}^{R\dagger} c_{k'-k}^R - c_{k'+k}^{R\dagger} c_{k'}^R) \\
&= \sum_{k'} v_F ((k'+k) c_{k'+k}^{R\dagger} c_{k'}^R - k' c_{k'+k}^{R\dagger} c_{k'}^R) \\
&= v_F k \rho_k
\end{aligned} \tag{47}$$

It turns out that the two equations (46) and (47) are in fact sufficient to determine the boson algebra and the bosonic representation of the Hamiltonian. In order to see this better we define conventional creation boson operators for positive k -values (i.e. shifting particles up $k > 0$)

$$b_k^{R\dagger} = i \sqrt{\frac{2\pi}{kN}} \rho_k^R, \tag{48}$$

while the hermitian conjugate annihilates an excitation by shifting particles down

$$b_k^R = -i\sqrt{\frac{2\pi}{kN}}\rho_{-k}^R \quad (49)$$

For left movers negative k -values correspond to an excitation, so that for $k > 0$

$$\rho_{-k}^L = \sum_{k'} c_{k'-k}^{L\dagger} c_{k'}^L = i\sqrt{\frac{kN}{2\pi}} b_k^{L\dagger} \quad (50)$$

The phase in the definition is in fact arbitrary, but we choose $\pm i$ for later convenience. Inserting this definition in (46) and (47) we recognize the canonical commutation relations

$$[b_k^R, b_{k'}^{R\dagger}] = \delta_{kk'}, \quad (51)$$

$$[H, b_k^{R\dagger}] = v_F k b_k^{R\dagger} \quad (52)$$

and likewise for left-movers. As shown in the treatment of the quantum harmonic oscillator in any quantum mechanics book, operators b^\dagger and b with such commutation relations are called creation and annihilation operators and can be used to build up the entire spectrum. In our case, we have such an oscillator spectrum for each $k > 0$ separately, describing the particle-hole excitations. Now, also taking the energy for adding/removing extra particles from equation (40) into account (see Fig. 16), we arrive at the complete Hamiltonian in bosonic form

$$H = v_F \sum_{k>0} k \left(b_k^{R\dagger} b_k^R + b_k^{L\dagger} b_k^L \right) + \frac{\pi v_F}{N} (n_R^2 + n_L^2) \quad (53)$$

where $(n_R^2 + n_L^2) \pi v_F / N$ is the energy in the first step of adding particles expressed in counting operators n_R and n_L (so-called *zero modes*) and $v_F k \left(b_k^{R\dagger} b_k^R + b_k^{L\dagger} b_k^L \right)$ corresponds to the second step of shifting of particles (so-called *oscillator modes*).

2.4 Fermion operators in terms of bosons

We have achieved the most important step of expressing the Hamilton operator entirely in terms of bosons. However, if we wish to calculate any physical expectation value we must also be able to express more general fermion operators in terms of the bosons. The bosons are well defined in terms of the fermions by equations (48-50), but we now seek the inverse transformation.

2.4.1 Left- and right-moving fermion densities

Using the concept of left- and right moving fermion field operators in equation (35) we can immediately define a corresponding left and right moving fermion density

$$\rho_R(x) = \psi_R^\dagger(x)\psi_R(x). \quad (54)$$

Technically this operator is divergent because the ground state expectation value is

$$\langle \rho_R(x) \rangle = \frac{1}{\ell} \sum_{k,k'} e^{-ikx/a} e^{ik'x/a} \langle c_k^{R\dagger} c_{k'}^R \rangle = \frac{1}{\ell} \sum_{k=-\infty}^0 \langle c_k^{R\dagger} c_k^R \rangle = \infty, \quad (55)$$

where we have used (35). However, we understand again that this infinity comes from introducing unphysical states below the lower cutoff $k < -\Lambda$ as discussed above. Since those states are always occupied, the same divergence will appear whenever this operator is applied on any physical state. However, we can simply remove the divergence by subtracting the ground state expectation value

$$: \rho_R(x) : = \psi_R^\dagger(x)\psi_R(x) - \langle \rho_R(x) \rangle \quad (56)$$

This procedure of subtracting the ground state expectation value is called *normal ordering* and is indicated by the dots at the sides. This definition is indeed useful because we are actually only interested in excitations on top of the well-defined ground state, namely the filled Fermi-sea. The normal ordered left- and right-moving densities therefore measure density-fluctuations relative to the ground state. Instead of subtracting the ground state expectation value, we can equivalently always re-order the plane-wave fermionic operators $c_k^{R\dagger}$ and c_k^R , so that the annihilation operators are to the right for $k > 0$ and to the left for $k \leq 0$ while keeping possible minus signs from the anti-commutator, i.e.

$$: c_k^{R\dagger} c_{k'}^R := - : c_{k'}^R c_k^{R\dagger} := \begin{cases} c_k^{R\dagger} c_{k'}^R & \text{for } k > 0 \\ -c_{k'}^R c_k^{R\dagger} & \text{for } k \leq 0 \end{cases} \quad (57)$$

Note, that the normal ordering can be omitted if $k \neq k'$, since $: c_k^{R\dagger} c_{k'}^R := c_k^{R\dagger} c_{k'}^R = -c_{k'}^R c_k^{R\dagger}$ already follows from the regular anti-commutation relations in that case. For normal ordered left movers the annihilation operators are to the left for $k > 0$ and to the right otherwise.

We now consider the Fourier transformation of the left- and right-moving densities, first

assuming $k \neq 0$. By using (35) and $\int_0^\ell dx e^{ikx/a} = \ell \delta_{k,0}$ we find

$$\begin{aligned}
\int_0^\ell e^{ikx/a} dx : \rho_R(x) : &= \frac{1}{\ell} \int_0^\ell dx \sum_{k''k'} e^{ikx/a} e^{-ik''x/a} e^{ik'x/a} : c_{k''}^{R\dagger} c_{k'}^R : \\
&= \sum_{k'} : c_{k+k'}^{R\dagger} c_{k'}^R : = \sum_{k'} c_{k+k'}^{R\dagger} c_{k'}^R \\
&= \rho_k^R
\end{aligned} \tag{58}$$

On the second line we used the fact that the normal ordering in (57) does not affect the expression for $k \neq 0$. We therefore find that the Fourier components of the right moving densities correspond exactly to the fermion shifting operators defined in (41)!

For $k = 0$ we have

$$\begin{aligned}
\int_0^\ell dx : \rho_R(x) : &= \frac{1}{\ell} \int_0^\ell dx \sum_{k''k'} e^{-ik''x/a} e^{ik'x/a} : c_{k''}^{R\dagger} c_{k'}^R : \\
&= \sum_{k'} : c_{k'}^{R\dagger} c_{k'}^R : \\
&= \sum_{k'>0} c_{k'}^{R\dagger} c_{k'}^R - \sum_{k'\leq 0} c_{k'}^R c_{k'}^{R\dagger} \\
&= n_R
\end{aligned} \tag{59}$$

We therefore find that the *zero mode* $:\rho_0^R:$ corresponds to the total number of right moving fermions relative to the ground state $:\rho_0^R := n_R$ (the third line corresponds to the number of excited particles $k'>0$ minus the number of holes $k'\leq 0$). In terms of the bosons in (48) the equations (58) and (59) can be summarized as

$$\int_0^\ell dx e^{ikx/a} : \rho_R(x) : = \sum_{k'} : c_{k'+k}^{R\dagger} c_{k'}^R := \begin{cases} -i\sqrt{\frac{kN}{2\pi}} b_k^{R\dagger} & \text{for } k > 0 \\ n_R & \text{for } k = 0 \\ i\sqrt{\frac{kN}{2\pi}} b_k^R & \text{for } k < 0 \end{cases} \tag{60}$$

We now make use of the inverse Fourier transform of equations (58) and (59), which is given by ($k = 2\pi n/N$)

$$\begin{aligned}
: \rho_R(x) : &= \frac{1}{\ell} \sum_k : \rho_k^R : e^{-ikx/a} = \frac{1}{\ell} \sum_{k>0} \sqrt{\frac{kN}{2\pi}} \left(i b_k^R e^{ikx/a} - i b_k^{R\dagger} e^{-ikx/a} \right) + \frac{n_R}{\ell} \\
&= \frac{1}{\ell} \sum_{n=1}^{\infty} \sqrt{n} \left(i b_n^R e^{i\frac{2\pi}{\ell} nx} - i b_n^{R\dagger} e^{-i\frac{2\pi}{\ell} nx} \right) + \frac{n_R}{\ell}
\end{aligned} \tag{61}$$

For the left moving density we can make the analogous calculations to find

$$\begin{aligned}
:\rho_L(x): &= \frac{1}{\ell} \sum_{k>0} \sqrt{\frac{kN}{2\pi}} \left(ib_k^{L\dagger} e^{ikx/a} - ib_k^L e^{-ikx/a} \right) + \frac{n_L}{\ell} \\
&= \frac{1}{\ell} \sum_{n=1}^{\infty} \sqrt{n} \left(ib_n^{L\dagger} e^{i\frac{2\pi}{\ell}nx} - ib_n^L e^{-i\frac{2\pi}{\ell}nx} \right) + \frac{n_L}{\ell}
\end{aligned} \tag{62}$$

In summary, we have derived central bosonization formulas which can be used in order to express fermionic densities in terms of bosons.

2.4.2 Boson field operator

It turns out to be useful to introduce a boson field operator ϕ_R in order to express the bosonization formulas (61) and (62) more compactly and also in order to make contact with conventional bosonic field theories. Let us define the fields ϕ_R and ϕ_L

$$\begin{aligned}
\phi_R(x) &= \phi_0^R + Q_R \frac{x}{\ell} + \sum_{n=1}^{\infty} \frac{1}{\sqrt{4\pi n}} \left(e^{i\frac{2\pi n}{\ell}x} b_n^R + e^{-i\frac{2\pi n}{\ell}x} b_n^{R\dagger} \right) \\
\phi_L(x) &= \phi_0^L + Q_L \frac{x}{\ell} + \sum_{n=1}^{\infty} \frac{1}{\sqrt{4\pi n}} \left(e^{-i\frac{2\pi n}{\ell}x} b_n^L + e^{i\frac{2\pi n}{\ell}x} b_n^{L\dagger} \right)
\end{aligned} \tag{63}$$

in terms of the boson operators $b_n^{R/L\dagger}$ and $b_n^{R/L}$ as defined in equations (48) and (50). The operators $Q_R = \sqrt{\pi}n_R$ and $Q_L = \sqrt{\pi}n_L$ measure the right- and left-moving particle number n_R and n_L . The operators ϕ_0^R and ϕ_0^L are defined as the canonical conjugate to the number operators

$$\begin{aligned}
[\phi_0^R, Q_R] &= -\frac{i}{2} \\
[\phi_0^L, Q_L] &= \frac{i}{2}
\end{aligned} \tag{64}$$

The definition in equation (63) is useful, because we can immediately express the fermion density in equations (61) and (62) as the derivative of the boson field ϕ_R and ϕ_L

$$\begin{aligned}
:\rho_R(x): &= \frac{1}{\sqrt{\pi}} \partial_x \phi_R(x) \\
:\rho_L(x): &= \frac{1}{\sqrt{\pi}} \partial_x \phi_L(x)
\end{aligned} \tag{65}$$

Moreover, the Hamiltonian can also be expressed in terms of the boson field as

$$H = av_F \int_0^\ell dx \left((\partial_x \phi_R)^2 + (\partial_x \phi_L)^2 \right) \quad (66)$$

Inserting the definition and using $\frac{1}{\ell} \int_0^\ell dx e^{i\frac{2\pi}{\ell}nx} = \delta_{n,0}$ we find that

$$H = \frac{2\pi v_F}{N} \sum_{n=1}^{\infty} n \left(b_n^{R\dagger} b_n^R + b_n^{L\dagger} b_n^L \right) + \frac{v_F}{N} (Q_R^2 + Q_L^2) \quad (67)$$

which indeed is identical to the boson expression we found in equation (53).

2.4.3 Fermion field

In order to express arbitrary fermion operators and calculate Green's functions, it is necessary to describe the fermion fields $\psi_R(x)$ and $\psi_L(x)$ in terms of bosons. We know that a right-moving fermion field $\psi_R(x)$ annihilates a fermion locally at position x and therefore changes the density $\rho_R(x) = \psi_R^\dagger(x)\psi_R(x)$ at that point. This action is reflected by the following commutation relation

$$\begin{aligned} [\psi_R(x), \rho_R(x')] &= \psi_R(x)\psi_R^\dagger(x')\psi_R(x') - \psi_R^\dagger(x')\psi_R(x')\psi_R(x) \\ &= \left\{ \psi_R(x), \psi_R^\dagger(x') \right\} \psi_R(x') \\ &= \delta(x - x')\psi_R(x) \end{aligned} \quad (68)$$

Our goal is therefore to find a bosonic expression for $\psi_R(x)$ which reproduces the commutation relation (68). The bosonic expression for the density $:\rho_R(x):$ is already known from equation (61).

Before we go further, let us review a general relation for commutators of two operators A and B . Assuming that $[[A, B], A] = 0$ we can show that

$$[e^A, B] = \sum_{n=1}^{\infty} \frac{1}{n!} [A^n, B] = \sum_{n=1}^{\infty} \frac{1}{n!} n A^{n-1} [A, B] = e^A [A, B] \quad (69)$$

Applying this equation to typical boson operators, i.e. $A=b, B=b^\dagger$ with $[A, B] = 1$, we get

$$\begin{aligned} [e^{\alpha b}, b^\dagger] &= \alpha e^{\alpha b} \\ [e^{\beta b^\dagger}, b] &= -\beta e^{\beta b^\dagger} \end{aligned} \quad (70)$$

The commutator with an exponential of boson operators is again proportional to the exponential which is approximately what we want in equation (68). We are therefore motivated to try

the following ansatz to describe the fermion field with an exponential of a linear combination of boson operators with arbitrary coefficients α_n and β_n

$$\psi_R(x) \propto \exp \left(\sum_{n>0} \left(\alpha_n(x) b_n^R + \beta_n(x) b_n^{R\dagger} \right) \right) \quad (71)$$

Using $[b_n^R, b_{n'}^{R\dagger}] = \delta_{n,n'}$ and for each index n, n' , we get

$$\begin{aligned} [\psi_R(x), b_n^{R\dagger}] &= \alpha_n \psi_R(x) \\ [\psi_R(x), b_n^R] &= -\beta_n \psi_R(x) \end{aligned} \quad (72)$$

Together with equation (61) we can therefore calculate the commutator

$$\begin{aligned} [\psi_R(x), \rho_R(x')] &= \frac{1}{\ell} \sum_{n=1}^{\infty} i\sqrt{n} \left(e^{i\frac{2\pi n}{\ell}x'} [\psi_R(x), b_n^R] - e^{-i\frac{2\pi n}{\ell}x'} [\psi_R(x), b_n^{R\dagger}] \right) \\ &= -\frac{1}{\ell} \sum_{n=1}^{\infty} i\sqrt{n} \left(\beta_n e^{i\frac{2\pi n}{\ell}x'} + \alpha_n e^{-i\frac{2\pi n}{\ell}x'} \right) \psi_R(x) \end{aligned} \quad (73)$$

So $[\psi_R(x), \rho_R(x)]$ is indeed proportional to $\psi_R(x)$ as desired. According to (68) we must choose the coefficients so that we get a delta function

$$-\frac{i}{\ell} \sum_{n=1}^{\infty} \sqrt{n} \left(\beta_n e^{i\frac{2\pi n}{\ell}x'} + \alpha_n e^{-i\frac{2\pi n}{\ell}x'} \right) = \delta(x - x'). \quad (74)$$

Comparing with the equation $\frac{1}{\ell} \sum_{n=-\infty}^{+\infty} e^{-i\frac{2\pi}{\ell}n(x-x')} = \delta(x - x')$, we conclude that

$$\alpha_n = \frac{i}{\sqrt{n}} e^{i\frac{2\pi}{\ell}nx} \quad \beta_n = \frac{i}{\sqrt{n}} e^{-i\frac{2\pi}{\ell}nx} \quad (75)$$

This reproduces the delta function almost perfectly, up to the $n = 0$ term. We therefore guess that we need the zero mode in the exponential ansatz (71) as well. From equations (64) and (69) we know

$$\left[e^{i\sqrt{4\pi}\phi_0^R}, \frac{Q_R}{\sqrt{\pi}} \right] = e^{i\sqrt{4\pi}\phi_0^R} \quad (76)$$

Therefore,

$$\psi_R(x) \propto \exp \left(i\sqrt{4\pi}\phi_0^R + \sum_{n>0} \frac{i}{\sqrt{n}} \left(e^{-i\frac{2\pi}{\ell}nx} b_n^{R\dagger} + e^{i\frac{2\pi}{\ell}nx} b_n^R \right) \right) \quad (77)$$

fulfills the relation

$$\begin{aligned}
[\psi_R(x), \rho_R(x)] &= \left[\psi_R(x), \frac{Q_R}{\ell\sqrt{\pi}} \right] + \frac{1}{\ell} \sum_{n=1}^{\infty} i\sqrt{n} \left(e^{i\frac{2\pi n}{\ell}x'} [\psi_R(x), b_n^R] - e^{-i\frac{2\pi n}{\ell}x'} [\psi_R(x), b_n^{R\dagger}] \right) \\
&= \left(\frac{1}{\ell} + \frac{1}{\ell} \sum_{n=1}^{\infty} (e^{i\frac{2\pi n}{\ell}(x'-x)} + e^{-i\frac{2\pi n}{\ell}(x'-x)}) \right) \psi_R(x) \\
&= \delta(x - x') \psi_R(x)
\end{aligned} \tag{78}$$

as required in equation (68). Including the operator Q_R in the exponential (77) does not change this relation, so that we can arrive at a compact form by comparison with (63)

$$\psi_R(x) \propto \exp\left(i\sqrt{4\pi}\phi_R(x)\right) \tag{79}$$

which is the famous bosonization formula for fermionic fields. Following the analog calculations for left-movers we find that

$$\psi_L(x) \propto \exp\left(-i\sqrt{4\pi}\phi_L(x)\right). \tag{80}$$

These two formulas will be useful when calculating Green's functions and general correlation functions as we will see later.

2.4.4 Field commutators

So far we have not specified the overall proportionality constant of the bosonization formulas (79) and (80). This can be fixed by using the proper normalization introduced in equation (37), but it must be noted here that even that normalization can in principle be chosen to be cutoff dependent, so that we could equally well leave the overall constant arbitrary, which is often done in the literature. Nonetheless, calculating the anti-commutator in bosonized form and calling the proportionality constant C , we get

$$\begin{aligned}
\left\{ \psi_R^\dagger(x), \psi_R(y) \right\} &= C^2 \left\{ e^{-i\sqrt{4\pi}\phi_R(x)}, e^{i\sqrt{4\pi}\phi_R(y)} \right\} \\
&= C^2 e^{-i\sqrt{4\pi}(\phi_R(x)-\phi_R(y))} \left(e^{2\pi[\phi_R(x),\phi_R(y)]} + e^{-2\pi[\phi_R(x),\phi_R(y)]} \right),
\end{aligned} \tag{81}$$

where we have used the so-called Baker Hausdorff formula

$$e^A e^B = e^{A+B} e^{\frac{1}{2}[A,B]} = e^B e^A e^{[A,B]} \tag{82}$$

(assuming $[[A, B], B] = [[A, B], A] = 0$). Hence we need to calculate the bosonic commutator (using (63) and (64))

$$\begin{aligned}
[\phi_R(x), \phi_R(y)] &= [Q_R, \phi_0^R] \left(\frac{x-y}{\ell} \right) \\
&\quad + \sum_{n, n'=1}^{\infty} \frac{1}{4\pi\sqrt{nn'}} \left(e^{i\frac{2\pi}{\ell}(nx-n'y)} [b_n^R, b_{n'}^{R\dagger}] + e^{-i\frac{2\pi}{\ell}(nx-n'y)} [b_n^{R\dagger}, b_{n'}^R] \right) \\
&= i\frac{x-y}{2\ell} + \sum_{n=1}^{\infty} \frac{1}{4\pi n} \left(e^{i\frac{2\pi n}{\ell}(x-y)} - e^{-i\frac{2\pi n}{\ell}(x-y)} \right) \\
&= i\frac{x-y}{2\ell} + \frac{1}{4\pi} \ln \left(1 - e^{-i\frac{2\pi}{\ell}(x-y)} \right) - \frac{1}{4\pi} \ln \left(1 - e^{i\frac{2\pi}{\ell}(x-y)} \right)
\end{aligned} \tag{83}$$

where we have used the expansion of the logarithm

$$\sum_{n=1}^{\infty} \frac{e^{-\alpha n}}{n} = -\ln(1 - e^{-\alpha}). \tag{84}$$

Since

$$\ln \left(\frac{1 - e^{-i\alpha}}{1 - e^{i\alpha}} \right) = \begin{cases} i(\pi - \alpha) & \text{for } \alpha > 0 \\ 0 & \text{for } \alpha = 0 \\ i(-\pi - \alpha) & \text{for } \alpha < 0 \end{cases}$$

we have

$$[\phi_R(x), \phi_R(y)] = \frac{i}{4} \text{sign}(x-y) = \begin{cases} \frac{i}{4} & \text{for } x-y > 0 \\ 0 & \text{for } x-y = 0 \\ -\frac{i}{4} & \text{for } x-y < 0 \end{cases} \tag{85}$$

Inserting this in equation (81) we get

$$\left\{ \psi_R^\dagger(x), \psi_R(y) \right\} = \begin{cases} 0 & \text{for } x \neq y \\ 2C^2 & \text{for } x = y \end{cases} \tag{86}$$

This expression agrees with (37) if the proportionality constant $C^2 = \delta(0)/2$ is chosen to be a delta function infinity (or alternatively is cutoff dependent, depending on the summation range in (37)).

Following the same steps for left movers, we find analogously

$$[\phi_L(x), \phi_L(y)] = -\frac{i}{4} \text{sign}(x-y) \tag{87}$$

Similarly, the anti-commutation relations between right- and left movers can be guaranteed

by demanding suitable commutation relations between the zero mode creation operators

$$[\phi_R^0, \phi_L^0] = \frac{i}{4}$$

which yields $[\phi_R(x), \phi_L(y)] = \frac{i}{4}$ and therefore $\{\psi_R(x), \psi_L(y)\} = 0$ according to equations (63) and (79). Alternatively, the commutation relations between left- and right-movers can also be fixed by using so-called Klein factors, which can also handle several fermion channels.

2.4.5 Bosonic excitation and zero modes

At this point it is useful to pause and look at the excitations of the bosonic Hilbert space in more detail. For the bosonic “oscillator” modes it is clear that the ground states of the Hamiltonian in (67) simply corresponds to the vacuum $|0\rangle$ which can be excited with an arbitrary number of bosons with the creation operators $b_n^{R\dagger}$ and $b_n^{L\dagger}$ for each n separately. The vacuum is defined as

$$b_n|0\rangle = 0 \quad \text{for all } n \quad (88)$$

The total fermion number relative to the ground state can be added and removed with the zero mode operators $\exp(-i\sqrt{4\pi}\phi_0^R)$ and $\exp(i\sqrt{4\pi}\phi_0^R)$, respectively. The corresponding relation $n_R e^{-i\sqrt{4\pi}\phi_0^R} |\lambda\rangle = e^{-i\sqrt{4\pi}\phi_0^R} (n_R + 1) |\lambda\rangle$ for any state $|\lambda\rangle$ can be shown with the help of equation (76) and is left as an exercise here (remember that $n_R = Q_R/\sqrt{\pi}$ is the counting operator). The fermion number creation always acts from below, i.e. the entire corresponding state is “pushed up” one step by acting with $\exp(-i\sqrt{4\pi}\phi_0^R)$ including any possible particle-hole excitations. An arbitrary number of fermions can be removed or added, but only in integer numbers (see also Fig. 16). The mathematical reason for this is actually the periodic boundary condition $\psi(x_j) = \psi(x_{j+N})$. According to equations (34) and (35) the boundary condition implies for the left and right moving fields

$$\psi_R(x) = \psi_R(x + \ell)e^{ik_F N}, \quad \psi_L(x) = \psi_L(x + \ell)e^{-ik_F N} \quad (89)$$

This translates into conditions on the boson field (63) by the use of the bosonization formula (79). Since the sum of oscillator modes in the boson field operator $\sum_{n=1}^{\infty} \frac{1}{\sqrt{4\pi n}} (e^{i\frac{2\pi n}{\ell}x} b_n^R + e^{-i\frac{2\pi n}{\ell}x} b_n^{R\dagger})$ is already periodic in ℓ , we are left with the following condition on the zero modes (using (82) since ϕ_0^R and Q_R do not commute):

$$\begin{aligned} e^{i\sqrt{4\pi}\phi_0^R} &= e^{i\sqrt{4\pi}(\phi_0^R + Q_R)} e^{ik_F N} = e^{i\sqrt{4\pi}\phi_0^R} e^{i\sqrt{4\pi}Q_R} e^{4\pi[\phi_0^R, Q_R]/2} e^{ik_F N} \\ \longrightarrow 1 &= e^{i\sqrt{4\pi}Q_R} e^{-i\pi} e^{ik_F N} \\ \longrightarrow \sqrt{4\pi}Q_R &= 2\pi n - k_F N + \pi \end{aligned} \quad (90)$$

We see that the number operator $Q_R/\sqrt{\pi} = n_R$ must indeed be an integer, since $k_F N = (n_0 + 1)\pi$ is an odd multiple of π according to equation (27). Therefore, zero mode particle excitations $\exp(-i\sqrt{4\pi}\phi_0^R)$ can only be added/removed in integral numbers. Arbitrary real numbers in the exponent would lead to unphysical states outside the Hilbert space. Interestingly, the spectrum and Hilbert-space of the zero modes therefore have a one-to-one correspondence to a single particle on a ring, where Q_R plays the role of the momentum operator and ϕ_0^R is the corresponding position operator with canonical commutation relations as defined in (64).

2.4.6 Summary of the bosonization formulas

Before we continue, let us summarize the most important bosonization formulas.

Linearization

$$c_k^R = c_{k_F+k} \quad c_k^L = c_{-k_F+k} \quad (32)$$

$$H = \sum_k v_F k \left(c_k^{R\dagger} c_k^R - c_k^{L\dagger} c_k^L \right) \quad (33)$$

$$\psi(x_j) = \sqrt{a} \left(e^{ik_F x_j/a} \psi_R(x_j) + e^{-ik_F x_j/a} \psi_L(x_j) \right) \quad (34)$$

$$\psi_R(x_j) = \frac{1}{\sqrt{\ell}} \sum_{k=-\infty}^{\infty} c_k^R e^{ikx_j/a} \quad \psi_L(x_j) = \frac{1}{\sqrt{\ell}} \sum_{k=-\infty}^{\infty} c_k^L e^{ikx_j/a} \quad (35)$$

Bosons in terms of fermions

$$-i\sqrt{\frac{kN}{2\pi}} b_k^{R\dagger} = \rho_k^R = \int_0^\ell : \rho_R(x) : e^{ikx/a} dx = \sum_{k'} c_{k'+k}^{R\dagger} c_{k'}^R \quad \text{for } k > 0 \quad (48)$$

$$i\sqrt{\frac{kN}{2\pi}} b_k^{L\dagger} = \rho_{-k}^L = \int_0^\ell : \rho_L(x) : e^{-ikx/a} dx = \sum_{k'} c_{k'-k}^{L\dagger} c_{k'}^L \quad \text{for } k > 0 \quad (50)$$

$$Q_{R/L}/\sqrt{\pi} = n_{R/L} = \int_0^\ell : \rho_{R/L}(x) : dx \quad (59)$$

$$H = v_F \sum_{k>0} k \left(b_k^{R\dagger} b_k^R + b_k^{L\dagger} b_k^L \right) + \frac{\pi v_F}{N} (n_R^2 + n_L^2) \quad (53)$$

Fermions in terms of bosons fields

$$: \rho_R(x) : = \frac{1}{\sqrt{\pi}} \partial_x \phi_R(x) \quad : \rho_L(x) : = \frac{1}{\sqrt{\pi}} \partial_x \phi_L(x) \quad (65)$$

$$\psi_R(x) \propto \exp(i\sqrt{4\pi}\phi_R(x)) \quad \psi_L(x) \propto \exp(-i\sqrt{4\pi}\phi_L(x)) \quad (79)$$

$$H = av_F \int_0^\ell dx \left((\partial_x \phi_R)^2 + (\partial_x \phi_L)^2 \right) \quad (66)$$

where

$$\phi_R(x) = \phi_0^R + Q_R \frac{x}{\ell} + \sum_{n=1}^{\infty} \frac{1}{\sqrt{4\pi n}} \left(e^{i\frac{2\pi n}{\ell} x} b_n^R + e^{-i\frac{2\pi n}{\ell} x} b_n^{R\dagger} \right) \quad (63)$$

$$\phi_L(x) = \phi_0^L + Q_L \frac{x}{\ell} + \sum_{n=1}^{\infty} \frac{1}{\sqrt{4\pi n}} \left(e^{-i\frac{2\pi n}{\ell} x} b_n^L + e^{i\frac{2\pi n}{\ell} x} b_n^{L\dagger} \right)$$

2.5 Correlation functions

As a typical application for bosonization, we would now like to calculate the correlation function for the fermion fields.

2.5.1 In space

Correlations along the wire decay according to the following expression

$$\langle \psi^\dagger(x)\psi(y) \rangle \approx ae^{-ik_F(x-y)/a} \langle \psi_R^\dagger(x)\psi_R(y) \rangle + ae^{ik_F(x-y)/a} \langle \psi_L^\dagger(x)\psi_L(y) \rangle \quad (91)$$

in the linearized approximation (34). The left and right movers are uncorrelated

$$\langle \psi_L^\dagger(x)\psi_R(y) \rangle = \langle \psi_R^\dagger(x)\psi_L(y) \rangle = 0,$$

because of the zero modes: If a right-mover is added $\exp(-i\sqrt{4\pi}\phi_0^R)$ it must also be removed again with $\exp(i\sqrt{4\pi}\phi_0^R)$ in order to get the ground state back. Therefore, in particular $\langle 0 | \exp(-i\sqrt{4\pi}\phi_0^R) | 0 \rangle = 0$.

Using the bosonization formula in real space we can write for the right moving correlation function (also using (82) and (85))

$$\begin{aligned} \langle \psi_R^\dagger(x)\psi_R(y) \rangle &= C^2 \langle e^{-i\sqrt{4\pi}(\phi_R(x)-\phi_R(y))} \rangle e^{2\pi[\phi_R(x),\phi_R(y)]} \\ &= C^2 \langle e^{-i\sqrt{4\pi}(\phi_R(x)-\phi_R(y))} \rangle e^{i\pi\text{sign}(x-y)/2} \end{aligned} \quad (92)$$

In order to calculate the expectation value of the exponential, we have to consider the zero modes and the oscillator modes separately. The expectation values of the zero modes are simple since the addition/removal operators cancel in the sum $\phi_R(x) - \phi_R(y)$ and we are left with

$$\langle 0 | \exp(-i\sqrt{4\pi}Q_R(x-y)/\ell) | 0 \rangle = 1 \quad (93)$$

which follows from the fact that the ground state has no additional particles $Q_R|0\rangle = 0$.

For the ground state expectation value of the oscillator modes we can use the Baker-Campbell-Hausdorff formula (82) in order to arrive at the general expression

$$\langle 0 | \exp(\alpha b + \beta b^\dagger) | 0 \rangle = \langle 0 | e^{\alpha b^\dagger} e^{\beta b} | 0 \rangle e^{\frac{\alpha\beta}{2}[b,b^\dagger]} = \exp(\alpha\beta/2) \quad (94)$$

where we have also used equation (88). In fact the relation (94) is just a special case for $T = 0$ of the more general cummulant theorem for bosons $\langle \exp(f) \rangle = \exp\langle f^2 \rangle / 2$ (see appendix equation (133)), which is valid for any temperature and any linear combination of bosons f as shown in the appendix. With the help of the cummulant formula (133) it is also possible to

calculate correlation functions at finite temperature and finite system sizes, which is explained in detail in Ref. [15] (also for “open” boundary conditions). For simplicity, we will restrict ourselves to the ground state correlation at $T = 0$.

Equation (92) can be evaluated by inserting the mode expansion (63) into (94)

$$\left\langle \psi_R^\dagger(x) \psi_R(y) \right\rangle = iC^2 \text{sign}(x-y) \left\langle e^{-\sum_n \frac{1}{2n} \left(e^{i\frac{2\pi}{\ell}nx} - e^{i\frac{2\pi}{\ell}ny} \right) \left(e^{-i\frac{2\pi}{\ell}nx} - e^{-i\frac{2\pi}{\ell}ny} \right)} \right\rangle \quad (95)$$

Using again the expansion of the logarithm (84), we find for the sum

$$\begin{aligned} \sum_{n>0} \frac{1}{n} \left(e^{i\frac{2\pi}{\ell}nx} - e^{i\frac{2\pi}{\ell}ny} \right) \left(e^{-i\frac{2\pi}{\ell}nx} - e^{-i\frac{2\pi}{\ell}ny} \right) \\ = \ln \left(1 - e^{i\frac{2\pi}{\ell}(x-y)} \right) + \ln \left(1 - e^{-i\frac{2\pi}{\ell}(x-y)} \right) - 2 \lim_{\varepsilon \rightarrow 0} (\ln \varepsilon) \end{aligned}$$

where the last term corresponds again to an infinity

$$\sum_{n=1}^{\infty} \frac{1}{n} = \lim_{\varepsilon \rightarrow 0} \sum_{n=1}^{\infty} \frac{e^{-\varepsilon n}}{n} = - \lim_{\varepsilon \rightarrow 0} \ln(1 - e^{-\varepsilon}) = - \lim_{\varepsilon \rightarrow 0} \ln \varepsilon. \quad (96)$$

However, this infinity combines with the prefactor C^2 , so that a finite result is obtained using the relation $\varepsilon C^2 = 1/\ell$.

$$\begin{aligned} \left\langle \psi_R^\dagger(x) \psi_R(y) \right\rangle &= \lim_{\varepsilon \rightarrow 0} iC^2 \text{sign}(x-y) \exp \left(\frac{1}{2} \ln \frac{\varepsilon}{1 - e^{i\frac{2\pi}{\ell}(x-y)}} \frac{\varepsilon}{1 - e^{-i\frac{2\pi}{\ell}(x-y)}} \right) \\ &= \frac{i}{2\ell} \frac{\text{sign}(x-y)}{\left| \sin \frac{\pi}{\ell}(x-y) \right|} \\ &= \frac{i}{2\ell \sin \frac{\pi}{\ell}(x-y)} \end{aligned} \quad (97)$$

The relation $\varepsilon C^2 = 1/\ell$ can be shown, e.g. by evaluating the correlation function (92) directly from the definition (35) by using the geometrical sum (and the quantization of the k -values relative to k_F as in equation (39)). The calculation for the left moving correlation function follows the same steps, except for a different sign in equation (87)

$$\left\langle \psi_L^\dagger(x) \psi_L(y) \right\rangle = - \frac{i}{2\ell \sin \frac{\pi}{\ell}(x-y)} \quad (98)$$

Therefore, in summary from equation (91)

$$\left\langle \psi^\dagger(x) \psi(y) \right\rangle = \frac{\sin k_F(x-y)}{N \sin \frac{\pi}{\ell}(x-y)} \quad (99)$$

It is left as an exercise for the reader to show that this is indeed the exact correlation function which can also be obtained without any approximations directly from (5).

2.5.2 In time

The time correlation function plays an important role, e.g. in order to evaluate the Green's function (17). Before we can evaluate the expectation values we have to determine how the operators evolve in time. Using the general formula

$$A(t) = e^{iHt} A e^{-iHt} \quad (100)$$

it is straightforward to show that

$$\begin{aligned} b_n^{R/L}(t) &= b_n^{R/L} e^{-in \frac{2\pi v_F}{N} t} \\ b_n^{R/L\dagger}(t) &= b_n^{R/L\dagger} e^{in \frac{2\pi v_F}{N} t} \\ Q_{R/L}(t) &= Q_{R/L} \\ \phi_0^{R/L}(t) &= \phi_0^{R/L} \mp Q_{R/L} \frac{v_F}{N} t \end{aligned} \quad (101)$$

Inserting these results into equation (63) we can immediately obtain a time-dependent mode expansion

$$\begin{aligned} \phi_R(x, t) &= \phi_0^R + Q_R \frac{x - av_F t}{\ell} + \sum_{n=1}^{\infty} \frac{1}{\sqrt{4\pi n}} \left(e^{i \frac{2\pi n}{\ell} (x - av_F t)} b_n^R + e^{-i \frac{2\pi n}{\ell} (x - av_F t)} b_n^{R\dagger} \right) \\ \phi_L(x, t) &= \phi_0^L + Q_L \frac{x + av_F t}{\ell} + \sum_{n=1}^{\infty} \frac{1}{\sqrt{4\pi n}} \left(e^{-i \frac{2\pi n}{\ell} (x + av_F t)} b_n^L + e^{i \frac{2\pi n}{\ell} (x + av_F t)} b_n^{L\dagger} \right) \end{aligned} \quad (102)$$

This is a remarkable result in many ways. First of all we see that the right- and left-movers are only functions of the right and left-moving light-cone coordinates $x \pm av_F t$. Secondly, with the help of this result the calculation of any time-space correlation function is no more or less difficult than the calculation of a pure space correlation function by substituting the time dependent light cone coordinates for $x - y$ in (97). That means that we have in principle the tools to solve any dynamic problem. In particular, we can immediately generalize the result (97) to express the time correlation function

$$\left\langle \psi_R^\dagger(t) \psi_R(0) \right\rangle = -\frac{i}{2\ell \sin \frac{\pi}{N} v_F t} \quad (103)$$

where it must be remembered that $t = \lim_{\varepsilon \rightarrow 0} (t - i\varepsilon)$ in order to ensure that the summation converges.

2.6 Spin-charge separation

One of the most famous and surprising results of one-dimensional many-body physics is the prediction of separate spin- and charge-excitations. We will show here that on the level of bosonization the spin-charge separation simply corresponds to taking suitable linear combinations of degenerate states.

2.6.1 Spin and charge excitations

All calculations that we have done so far actually also apply for electrons with spin if we use two species of bosons ϕ_σ with index $\sigma = \downarrow, \uparrow$, one for spin up and one for spin down. According to equation (65) the bosons can immediately be related to fermionic densities with spin up and spin down.

$$:\rho_{R/L}^\sigma(x): = \frac{1}{\sqrt{\pi}} \partial_x \phi_{R/L}^\sigma(x) \quad \sigma = \uparrow, \downarrow \quad (104)$$

If we are interested in the total charge density at a point x , we will use the sum of spin up and spin down

$$:\rho_{R/L}^c(x): =: \rho_{R/L}^\uparrow(x): +: \rho_{R/L}^\downarrow(x): \quad (105)$$

Likewise, we can calculate the total spin density at point x by using the difference

$$:\rho_{R/L}^s(x): =: \rho_{R/L}^\uparrow(x): -: \rho_{R/L}^\downarrow(x): \quad (106)$$

Analogously, we can define new boson fields that correspond to the spin and charge densities

$$\begin{aligned} \phi_{R/L}^c(x) &= \frac{1}{\sqrt{2}} \left(\phi_{R/L}^\uparrow(x) + \phi_{R/L}^\downarrow(x) \right) \\ \phi_{R/L}^s(x) &= \frac{1}{\sqrt{2}} \left(\phi_{R/L}^\uparrow(x) - \phi_{R/L}^\downarrow(x) \right) \end{aligned} \quad (107)$$

This defines new zero modes and oscillator mode operators (the index for left and right movers L/R is omitted here)

$$\begin{aligned} b_n^{c/s} &= \frac{1}{\sqrt{2}} \left(b_n^\uparrow \pm b_n^\downarrow \right) \\ \phi_0^{c/s} &= \frac{1}{\sqrt{2}} \left(\phi_0^\uparrow \pm \phi_0^\downarrow \right) \\ Q^{c/s} &= \frac{1}{\sqrt{2}} \left(Q^\uparrow \pm Q^\downarrow \right) \end{aligned} \quad (108)$$

which have again canonical commutation relations analogous to (51) and (64) as can easily be verified. The mode expansion of the fields (107) in terms of the new operators (108) is then the same as before.

It is a straightforward exercise to write the bosonization formulas (65) and (79) in terms

of the new spin and charge fields, for example:

$$\begin{aligned}
\psi_R^\uparrow(x) &\propto \exp\left(i\sqrt{4\pi}\phi_R^\uparrow(x)\right) = \exp i\sqrt{2\pi}(\phi_R^c(x) + \phi_R^s(x)) \\
:\rho_R^\downarrow(x): &:= \frac{1}{\sqrt{\pi}}\partial_x\phi_R^\downarrow(x) = \frac{1}{\sqrt{2\pi}}(\partial_x\phi_R^c(x) - \partial_x\phi_R^s(x)) \\
:\rho_R^{s/c}(x): &:= \sqrt{\frac{2}{\pi}}\partial_x\phi_R^{s/c}(x)
\end{aligned} \tag{109}$$

Most importantly, the Hamiltonian (66) can also be written in terms of the new spin and charge operators

$$\begin{aligned}
H &= av_F \int_0^\ell dx \left((\partial_x\phi_R^\uparrow)^2 + (\partial_x\phi_R^\downarrow)^2 + (\partial_x\phi_L^\uparrow)^2 + (\partial_x\phi_L^\downarrow)^2 \right) \\
&= av_F \int_0^\ell dx \left((\partial_x\phi_R^c)^2 + (\partial_x\phi_R^s)^2 + (\partial_x\phi_L^c)^2 + (\partial_x\phi_L^s)^2 \right)
\end{aligned} \tag{110}$$

Since the spin and charge excitations appear separately in the Hamiltonian (110), the partition function factorizes. It is therefore possible to regard the spin and charge particles as the “new” independent fundamental excitations instead of the “old” spin up and spin down particles. Indeed, because of the degeneracy of the spin up and spin down channel, we could have used any canonical rotation to define new particles, but spin and charge are particularly useful when interactions are present. This is intuitively clear because realistic interactions will couple total charge densities and thereby lift the degeneracy between the spin and the charge channel. With interactions we are therefore forced to use the picture of spin and charge excitations, since the freedom of rotating degenerate channels is lost.

It should be noted that the spin and charge separation is not obeyed exactly for the particle numbers, because the “new” zero modes still must obey the “old” quantization formula (90). In particular, the number of charge and spin particles is given by

$$\begin{aligned}
n_R^c &= n_R^\uparrow + n_R^\downarrow = \sqrt{\frac{2}{\pi}}Q_R^c \\
n_R^s &= n_R^\uparrow - n_R^\downarrow = \sqrt{\frac{2}{\pi}}Q_R^s
\end{aligned} \tag{111}$$

Both numbers must be integers, but cannot be changed independently. Adding a spin particle must always be accompanied by adding or removing a charge particle and vice versa, i.e. the total sum of spin and charge particles must always remain even. This just reflects the fact that we always have to add and remove real electrons, instead of spin/charge quasi-particles.

We are now in the position to also interpret the nature of the spin and charge excitations. As discussed in section 2.2 we understand the bosonic excitations in terms of fermions being

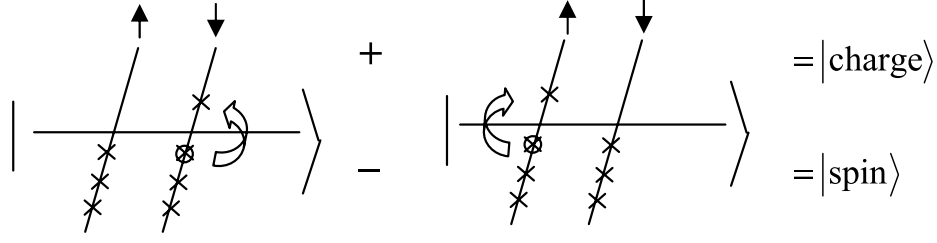


Figure 17: Charge excitations are symmetric linear combinations of up and down excitations. Spin excitations are anti-symmetric linear combinations of up and down.

shifted up the spectrum. The spin and charge excitation now simply correspond to odd and even linear combinations of those shifts according to equation (108). This is depicted schematically in diagram 17.

2.6.2 Spin and charge correlation functions

We now have the tools in order to calculate correlation functions of electrons with spin

$$\langle \psi^{\uparrow\dagger}(x)\psi^{\uparrow}(y) \rangle \approx ae^{-ik_F(x-y)} \langle \psi_R^{\uparrow\dagger}(x)\psi_R^{\uparrow}(y) \rangle + ae^{ik_F(x-y)} \langle \psi_L^{\uparrow\dagger}(x)\psi_L^{\uparrow}(y) \rangle$$

Using equation (109) we can calculate the right moving part (using the same calculations as in section 2.5)

$$\begin{aligned} \langle \psi_R^{\uparrow\dagger}(x)\psi_R^{\uparrow}(y) \rangle &\propto i \operatorname{sign}(x-y) \langle e^{-i\sqrt{4\pi}(\phi_R^{\uparrow}(x)-\phi_R^{\uparrow}(y))} \rangle \\ &= i \operatorname{sign}(x-y) \langle e^{-i\sqrt{2\pi}(\phi_R^c(x)-\phi_R^c(y))} \rangle \times \langle e^{-i\sqrt{2\pi}(\phi_R^s(x)-\phi_R^s(y))} \rangle \\ &= i \operatorname{sign}(x-y) \frac{1}{\sqrt{|\sin \frac{\pi(x-y)}{\ell}|}} \times \frac{1}{\sqrt{|\sin \frac{\pi(x-y)}{\ell}|}} \end{aligned} \quad (112)$$

Without interactions the outcome is of course identical to the spinless result (97), but the calculation shows that the correlation function factorizes into a spin and a charge part. When interactions are introduced in the next section we expect that the degeneracy of spin and charge is lifted and therefore the correlations decay differently and independently for spin- and charge-like excitations.

3 Electron-electron interactions

Finally we are now in the position to deal with interaction effects, which of course is the main goal of bosonization. After having derived the mathematical foundation of bosonization in the previous section, it is now straightforward to apply that prescription to typical interaction terms discussed above (see equations (9) and (10))

3.1 Scattering processes

Let us consider the standard model of density-density interactions in equation (9)

$$H_{\text{int}} = \sum_{j=1}^N \sum_{m=1}^N \psi^\dagger(x_j) \psi(x_j) U(m) \psi^\dagger(x_{j+m}) \psi(x_{j+m})$$

or equivalently in terms of the wave-numbers k in equation (10)

$$H_{\text{int}} = \frac{1}{N} \sum_{k, k', \Delta k} c_k^\dagger c_{k-\Delta k} U(\Delta k) c_{k'}^\dagger c_{k'+\Delta k}. \quad (113)$$

Following the standard program of bosonization, the first step is always to restrict the creation and annihilation operators in a linearized region $|k-k_F| < \Lambda$ and $|k+k_F| < \Lambda$ around k_F according to Fig. 14 (see section 2.1). Let us systematically analyze the different possibilities as shown in Fig. 18.

Forward scattering

We first consider the case of small momentum transfer $\Delta k < \Lambda$, which is commonly referred to as *forward scattering*, since a right mover is always scattered into a right mover and a left mover is always scattered into a left mover. Using equation (32) and restricting the momenta k and k' to left movers $-k_F - \Lambda < k$, $k' < -k_F + \Lambda$ or right movers $k_F - \Lambda < k$, $k' < k_F + \Lambda$, the corresponding interaction Hamiltonian is given by

$$\begin{aligned} H_{\text{forward}} &= \frac{1}{N} \sum_{k, k', \Delta k} \left(c_k^{R\dagger} c_{k-\Delta k}^R + c_{k'}^{L\dagger} c_{k'-\Delta k}^L \right) U(\Delta k) \left(c_{k'}^{R\dagger} c_{k'+\Delta k}^R + c_{k'}^{L\dagger} c_{k'+\Delta k}^L \right) \\ &= \frac{1}{N} \sum_{\Delta k=-\infty}^{\infty} \left(g_2 (\rho_{-\Delta k}^R \rho_{\Delta k}^L + \rho_{-\Delta k}^L \rho_{\Delta k}^R) + g_4 (\rho_{-\Delta k}^R \rho_{\Delta k}^R + \rho_{-\Delta k}^L \rho_{\Delta k}^L) \right) \\ &= \frac{1}{N} \sum_{n=1}^{\infty} \left(2ng_2 (b_n^{R\dagger} b_n^{L\dagger} + b_n^R b_n^L) + 2ng_4 (b_n^{R\dagger} b_n^R + b_n^{L\dagger} b_n^L) \right. \\ &\quad \left. + 2g_2 n_R n_L + g_4 (n_R^2 + n_L^2) + \text{const.} \right) \end{aligned} \quad (114)$$

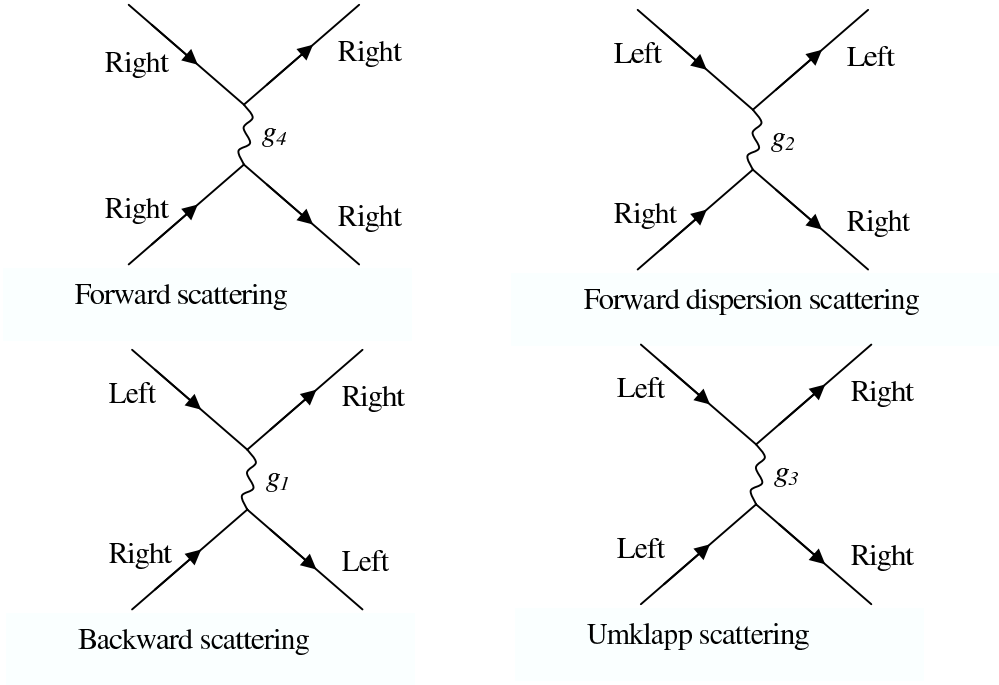


Figure 18: The different scattering processes in the linearized approximation.

where we have used equations (41) and (50). The constant comes from ordering the bosons and plays no significant role in the Hamiltonian. It is customary to denote the right-left interaction by $g_2 = U(\Delta k)$, which is sometimes also called dispersion scattering. The density-density interaction strength on the same branch is denoted by $g_4 = U(\Delta k)$. Often g_2 and g_4 are taken to be independent of momentum, which is justified for short range potentials $U(m)$ that drop off quickly for $m > 1/\Lambda$. In that case, we can write the forward scattering term more compactly with the help of equation (63)

$$H_{\text{forward}} = \frac{a}{\pi} \int_0^\ell dx \left(2g_2 (\partial_x \phi_R \partial_x \phi_L) + g_4 ((\partial_x \phi_R)^2 + (\partial_x \phi_L)^2) \right) \quad (115)$$

Backward scattering

There are additional terms in equation (10) corresponding to large momentum transfer around $\pm 2k_F$, which scatter left into right movers and vice versa. We use a new parameterization $\Delta k = \pm(2k_F + \delta k)$, where δk is now assumed to be small. Using (10) and (32), we

obtain

$$\begin{aligned}
H_{\text{backward}} &= \frac{1}{N} \sum_{k,k',\delta k} c_k^{R\dagger} c_{k-\delta k}^L U(2k_F + \delta k) c_{k'}^{L\dagger} c_{k'+\delta k}^R + c_k^{L\dagger} c_{k-\delta k}^R U(-2k_F - \delta k) c_{k'}^{R\dagger} c_{k'+\delta k}^L \\
&= \frac{1}{N} \sum_{k,k',\Delta k} g_1 \left(c_k^{R\dagger} c_{k+\Delta k}^R c_{k'-\Delta k}^L c_{k'}^{L\dagger} + c_k^{L\dagger} c_{k+\Delta k}^L c_{k'-\Delta k}^R c_{k'}^{R\dagger} \right)
\end{aligned}$$

where we have again re-parameterized $\Delta k = \delta k + k' - k$ in the last step and defined the backward scattering amplitude $g_1 = U(2k_F + \Delta k + k - k')$, which can be assumed to be approximately constant for k , k' and Δk on the range of the cutoff Λ in most cases. Therefore, using (41) and (50)

$$H_{\text{backward}} \approx \frac{1}{N} \sum_{k,k',\Delta k} g_1 (\rho_{\Delta k}^R \rho_{-\Delta k}^L + \rho_{\Delta k}^L \rho_{-\Delta k}^R) \quad (116)$$

which has the same effect as the dispersion scattering equation (114) above and therefore can be absorbed right away by a redefinition of the corresponding scattering amplitude g_2 . For electrons with spin the backward scattering also introduces a spin-flip term, which can be taken into account by a renormalization group treatment, but will not be addressed here.

Umklapp scattering

Finally, there is the possibility of Umklapp scattering of two left movers into two right movers and vice versa in case that $\Delta k = \pm(4k_F + \delta k) = \pm(2\pi + \delta k)$. This Umklapp scattering (denoted by g_3) is obviously only present if the special condition for half-filling $4k_F = 2\pi$ is fulfilled. The resulting operator can then also be bosonized with the help of the fermion field expressions (79) and (80), but we will not consider this special case here.

It should be noted here that the bosonization of the various scattering terms can also be derived from the interaction Hamiltonian in real space (9) by using the linearization formula (34) together with (65) if we assume a short range potential $U(m)$ (as can be verified as an exercise). However, the derivation in momentum space has the advantage that the k -dependence of the scattering amplitudes g_2 and g_4 can be preserved.

3.2 The Luttinger Liquid parameter: Bogoliubov transformation

The bosonized interaction Hamiltonian in (114) or (115) is much easier to treat than the fermionic version (9), because it is represented by terms that only involve a product of two boson operators (bilinear) as opposed to four fermion operators in (9) and (10). In fact, it is well known how to solve such problems by a suitable redefinition of the bosonic operators so that the interaction term has the same form as the original Hamiltonian, which only contains counting operators. This procedure is called a Bogoliubov transformation and is given by the

general ansatz

$$\begin{aligned}\tilde{b}_n^R &= b_n^R \cosh \theta - b_n^{L\dagger} \sinh \theta \\ \tilde{b}_n^L &= b_n^L \cosh \theta - b_n^{R\dagger} \sinh \theta\end{aligned}\tag{117}$$

which defines new operators \tilde{b}_n^R and \tilde{b}_n^L . It is left as an exercise to show that those new operators also obey the canonical commutation relations (51).

We notice that the g_4 interaction in (114) or (115) is already in the non-interacting form of equations (66) and (67) and can be absorbed right away by defining a new Fermi velocity

$$\tilde{v}_F = v_F + \frac{g_4}{\pi}\tag{118}$$

Therefore the complete Hamiltonian can be written as

$$\begin{aligned}H &= a\tilde{v}_F \int_0^\ell dx \left((\partial_x \phi_R)^2 + (\partial_x \phi_L)^2 + \frac{2g_2}{\tilde{v}_F \pi} \partial_x \phi_R \partial_x \phi_L \right) \\ &= \sum_{n=1}^{\infty} \frac{2\pi\tilde{v}_F}{N} n \left(b_n^{R\dagger} b_n^R + b_n^{L\dagger} b_n^L + \frac{g_2}{\tilde{v}_F \pi} (b_n^{R\dagger} b_n^{L\dagger} + b_n^R b_n^L) \right) \\ &\quad + \frac{\tilde{v}_F}{N} \left(Q_R^2 + Q_L^2 + \frac{2g_2}{\tilde{v}_F \pi} Q_R Q_L \right)\end{aligned}\tag{119}$$

(where g_2 is assumed to contain also any possible backward scattering contributions (116)). It is clear now that we want to use the canonical transformation (117) in order to get rid of the cross terms $b_n^{R\dagger} b_n^{L\dagger} + b_n^R b_n^L$. This can be done by comparing with the following expression (up to a constant)

$$\tilde{b}_n^{R\dagger} \tilde{b}_n^R + \tilde{b}_n^{L\dagger} \tilde{b}_n^L = (\cosh^2 \theta + \sinh^2 \theta) (b_n^{R\dagger} b_n^R + b_n^{L\dagger} b_n^L) - 2 \cosh \theta \sinh \theta (b_n^{L\dagger} b_n^{R\dagger} + b_n^L b_n^R)\tag{120}$$

which yields the following result for the rotation angle θ

$$K = e^{2\theta} = \sqrt{\frac{1 - g_2/v_F \pi}{1 + g_2/v_F \pi}}\tag{121}$$

where K is the so called *Luttinger liquid parameter*. It is straightforward to verify this result using the following formulas

$$\begin{aligned}\sinh \theta &= \frac{1}{2} (\sqrt{K} - 1/\sqrt{K}) & \cosh \theta &= \frac{1}{2} (\sqrt{K} + 1/\sqrt{K}) & \sinh \theta + \cosh \theta &= \sqrt{K} \\ \sinh^2 \theta + \cosh^2 \theta &= (K + 1/K)/2 & 2 \sinh \theta \cosh \theta &= (K - 1/K)/2\end{aligned}\tag{122}$$

Likewise, we can define new number operators

$$\begin{aligned}\tilde{Q}_R &= Q_R \cosh \theta - Q_L \sinh \theta \\ \tilde{Q}_L &= Q_L \cosh \theta - Q_R \sinh \theta\end{aligned}\tag{123}$$

after which the Hamiltonian is in the standard form again

$$\begin{aligned}H &= \sum_{n=1}^{\infty} \frac{2\pi\tilde{v}_F}{N} n \left(\tilde{b}_n^{R\dagger} \tilde{b}_n^R + \tilde{b}_n^{L\dagger} \tilde{b}_n^L \right) + \frac{\tilde{v}_F}{N} \left(\tilde{Q}_R^2 + \tilde{Q}_L^2 \right) \\ &= a\tilde{v}_F \int_0^\ell dx \left((\partial_x \tilde{\phi}_R)^2 + (\partial_x \tilde{\phi}_L)^2 \right),\end{aligned}\tag{124}$$

where we have also defined new fields $\tilde{\phi}_R$ and $\tilde{\phi}_L$ analogous to equations (117) and (123). More compactly we can summarize these formulas in a canonical rescaling equation for the difference and the sum of the left and right moving fields

$$\begin{aligned}\tilde{\phi}_R - \tilde{\phi}_L &= \sqrt{K}(\phi_L - \phi_R) \\ \tilde{\phi}_R + \tilde{\phi}_L &= \frac{1}{\sqrt{K}}(\phi_L + \phi_R)\end{aligned}\tag{125}$$

This implies also that the creation operators $\tilde{\phi}_0^R$ and $\tilde{\phi}_0^L$ are transformed, but it should be remembered that the quantization relation must still be fulfilled and particle excitations are performed by the “old” operator $\exp(-i\sqrt{4\pi}\phi_0^R)$.

In summary, we have therefore solved an interacting problem exactly by a simple canonical transformation. Moreover, all interactions can be described by a single *Luttinger liquid parameter* $K = e^{2\theta}$ in equation (121). Even though K can in principle be dependent on the momentum transfer $k = n2\pi/N$ it is often sufficient to just use a constant value for short range interacting models. However, it turns out that the expression is only correct to lowest order in the actual scattering amplitudes g_2 in typical lattice Hamiltonians like nearest neighbor interactions or the Hubbard model [16], because higher order operators renormalize the interactions. Therefore, the actual value of the Luttinger liquid parameter K must almost always be inferred from other theoretical methods [16,17] or by comparisons with experiments. For repulsive interactions we see from equation (121) that $K < 1$. For $K = 1$ we recover the non-interacting theory.

3.3 Correlation functions

To conclude this chapter, we would now like to apply our solution of the problem in order to calculate correlation functions in an interacting model. Again starting from (91) we are

interested in the correlator of the right moving field $\psi_R \propto e^{i\sqrt{4\pi}\phi_R(x)} = e^{i\sqrt{4\pi}(\tilde{\phi}_R \cosh \theta + \tilde{\phi}_L \sinh \theta)}$. In particular,

$$\begin{aligned} \langle \psi_R^\dagger(x) \psi_R(y) \rangle &\propto e^{2\pi[\phi_R(x), \phi_R(y)]} \langle e^{-i\sqrt{4\pi}(\phi_R(x) - \phi_R(y))} \rangle \\ &= e^{i\pi \text{sign}(x-y)/2} \langle e^{-i\sqrt{4\pi}(\tilde{\phi}_R(x) - \tilde{\phi}_R(y)) \cosh \theta} \rangle \langle e^{-i\sqrt{4\pi}(\tilde{\phi}_L(x) - \tilde{\phi}_L(y)) \sinh \theta} \rangle \end{aligned}$$

where we have used (79) and (117). The transformed operators $\tilde{\phi}_R$ and $\tilde{\phi}_L$ have the same canonical mode expansion as before and therefore the calculation of the correlation functions proceeds as in section 2.5.

In contrast to equation (97), however, the overall proportionality constant is now cut-off dependent and not normalized to unity. The left moving correlator differs by a minus sign.

$$\begin{aligned} \langle \psi_R^\dagger(x) \psi_R(y) \rangle &\propto i \text{sign}(x-y) \left| 2\ell \sin \frac{\pi}{\ell}(x-y) \right|^{-\cosh^2 \theta} \left| 2\ell \sin \frac{\pi}{\ell}(x-y) \right|^{-\sinh^2 \theta} \\ &\propto i \text{sign}(x-y) \left| 2\ell \sin \frac{\pi}{\ell}(x-y) \right|^{-(K+1/K)/2} \end{aligned} \quad (126)$$

As in section 2.5 we can also use the time dependent mode expansion in order to calculate the Green's function. Accordingly, we find

$$\langle \psi_R^\dagger(t) \psi_R(0) \rangle \propto i \text{sign}(t) \left| 2\ell \sin \frac{\pi v_F a t}{\ell} \right|^{-(K+1/K)/2} \quad (127)$$

A famous result for the density of states can now be obtained in the thermodynamic limit $\ell \rightarrow \infty$, since according to equations (17) and (127)

$$G^R(t, x) = -i \langle \{ \psi(x, t), \psi^\dagger(x, 0) \} \rangle \theta(t) \stackrel{\ell \rightarrow \infty}{\propto} t^{-(K+1/K)/2} \quad (128)$$

and therefore from the density of state becomes,

$$\rho(\omega) \propto \int dt e^{i\omega t} t^{-(K+1/K)/2} \propto \omega^{(K+1/K)/2-1}. \quad (129)$$

where we have simply used a rescaling of the integration variable $x = \omega t$. This is the famous result of the depletion at low frequencies of the single particle spectral weight in a Luttinger liquid with a characteristic power-law

$$\rho(\omega) \propto \omega^\alpha, \quad \alpha = \frac{K+1/K-2}{2} > 0 \quad (130)$$

This depletion is one of the main hallmarks which is used in order to detect Luttinger liquid behavior experimentally with tunneling and photoemission experiments [7–9] as described

in section 1.2. It must be emphasized again that the proportionality constant is not known, but tunneling experiments cannot detect the overall amplitude of the density of states either. Theoretically it is possible to describe the proportionality constant of correlators phenomenologically with a cut-off energy scale [1–5] or by using a restricted momentum range for the interactions [18], but these are just mathematical tools that do not determine the actual value. In some microscopic models it is possible to fix the proportionality constant and the Luttinger liquid parameter by comparison with other exact methods [16, 17, 19].

As mentioned above, the correlators for electrons with spin factorize in a spin part and a charge part. In this case the interactions only transform the charge bosons unless spin-dependent scattering is considered. Therefore, we can immediately generalize equation (112) for the interacting case

$$\langle \psi_R^{\uparrow\uparrow}(x) \psi_R^{\uparrow}(y) \rangle \propto i \operatorname{sign}(x - y) \left| 2\ell \sin \frac{\pi(x + y)}{\ell} \right|^{-1/2} \left| 2\ell \sin \frac{\pi(x - y)}{\ell} \right|^{-(K+1/K)/4} \quad (131)$$

and analogously for the time correlations. The corresponding result for the power-law depletion of the density of states becomes analogous to (129) and (130)

$$\rho(\omega) \propto \omega^\alpha, \quad \alpha = \frac{K + 1/K - 2}{4} > 0 \quad (132)$$

If a general correlation in space and time is calculated, the two factors in (131) contain different velocities $v_c > v_s$, corresponding to the separate excitations of spin and charge.

This concludes the elementary introduction to bosonization. Using the tools we have developed here the reader is encouraged to explore also some of the more advanced topics, which can for example be found in the suggested review articles [1–5].

4 Appendix: The boson cummulant formula

The cummulant formula for bosons states that the finite temperature expectation value of an exponential of a linear combination of boson creation and annihilation operators can be expressed as the exponential of an expectation value in the following way

$$\langle e^{\alpha b + \beta b^\dagger} \rangle = e^{\langle (\alpha b + \beta b^\dagger)^2 \rangle / 2} \quad (133)$$

If more than one species of bosons is present, this expression factorizes on both sides so that it can be used for any linear combination of bosons $f = \sum_n (\alpha_n b_n + \beta_n b_n^\dagger)$. It is not valid for the zero-mode operators, however (see Ref. [15] for a discussion on finite temperature expectation values of zero modes).

The right hand side of equation (133) can be evaluated rather easily by use of the Bose-Einstein distribution for finite temperatures $\beta=1/k_B T$ in terms of the corresponding energy quantum $\hbar\omega$

$$\langle b^\dagger b \rangle = \frac{\sum_{n=0}^{\infty} e^{-n\beta\hbar\omega} \langle n | b^\dagger b | n \rangle}{\sum_{n=0}^{\infty} e^{-n\beta\hbar\omega}} = \frac{e^{-\beta\hbar\omega}}{e^{-\beta\hbar\omega} - 1}$$

Therefore,

$$\begin{aligned} e^{\langle(\alpha b + \beta b^\dagger)^2\rangle/2} &= e^{\alpha\beta\langle bb^\dagger + b^\dagger b\rangle/2} \\ &= e^{\alpha\beta\langle b^\dagger b\rangle + \alpha\beta[b, b^\dagger]/2} \\ &= e^{\frac{\alpha\beta q}{1-q} + \frac{\alpha\beta}{2}} \\ &= e^{-\alpha\beta/2} e^{\frac{\alpha\beta}{1-q}} \end{aligned} \tag{134}$$

where we have introduced the Boltzmann weight $q = \exp(-\beta\hbar\omega)$.

For the left hand side of (133) we use the Baker Hausdorff formula (82) and expand the exponential

$$\begin{aligned} \langle e^{\alpha b + \beta b^\dagger} \rangle &= \langle e^{\alpha b} e^{\beta b^\dagger} \rangle e^{\alpha\beta[b^\dagger, b]/2} \\ &= e^{-\alpha\beta/2} \sum_{n, n'=0}^{\infty} \frac{\alpha^n \beta^{n'}}{n! n'!} \langle b^n b^{n'\dagger} \rangle \\ &= e^{-\alpha\beta/2} \sum_{n=0}^{\infty} \frac{(\alpha\beta)^n}{(n!)^2} \frac{\sum_{m=0}^{\infty} q^m \langle m | b^n b^{n\dagger} | m \rangle}{\sum_{m=0}^{\infty} q^m} \\ &= (1-q) e^{-\alpha\beta/2} \sum_{n=0}^{\infty} \frac{(\alpha\beta)^n}{(n!)^2} \sum_{m=0}^{\infty} q^m \langle m | b^n b^{n\dagger} | m \rangle \end{aligned} \tag{135}$$

where we have used the standard expression for a temperature expectation value with the Boltzmann weight q . For a harmonic oscillator it is well known that the expectation value in the m^{th} excited state is given by

$$\langle m | b^n b^{n\dagger} | m \rangle = \frac{(m+n)!}{m!}$$

(e.g. by repeated use of $b^\dagger |m\rangle = \sqrt{m+1} |m+1\rangle$). Finally, we insert into equation (135) the following Taylor expansion around $q = 0$

$$(1-q)^{-n-1} = \sum_{m=0}^{\infty} q^m \frac{(m+n)!}{n! m!}$$

(which can be verified by repeated differentiation). Therefore, equation (135) becomes

$$\begin{aligned} \langle e^{\alpha b + \beta b^\dagger} \rangle &= (1-q)e^{-\alpha\beta/2} \sum_{n=0}^{\infty} \frac{(\alpha\beta)^n}{n!} (1-q)^{-n-1} \\ &= e^{-\alpha\beta/2} \sum_{n=0}^{\infty} \frac{1}{n!} \left(\frac{\alpha\beta}{1-q} \right)^n \\ &= e^{-\alpha\beta/2} \exp\left(\frac{\alpha\beta}{1-q} \right) \end{aligned}$$

which is exactly the same expression as on the left hand side (134) and therefore concludes the proof of the cumulant theorem. Note that at $T = 0$, we have $q = \exp(-\beta\hbar\omega) \rightarrow 0$, so that

$$\langle e^{\alpha b + \beta b^\dagger} \rangle = e^{\langle (\alpha b + \beta b^\dagger)^2 \rangle / 2} = \exp\left(\frac{\alpha\beta}{2} \right)$$

as already shown in equation (94) .

References

- [1] F.D.M. Haldane, “Luttinger liquid theory’ of one-dimensional quantum fluids”, J. Phys. C: Solid State Phys. **14**, 2585 (1981)
- [2] J.Voit, “One dimensional Fermi liquids”, Rep. Prog. Phys. **58** (1995); cond-mat/9510014.
- [3] H.J. Schultz, G. Cuniberti, P. Pieri, in “*Field Theories for Low-Dimensional Condensed Matter System*”. G. Morandi et al. (Eds.), Springer (2000); preprint cond-mat/9807366
- [4] A.O. Gogolin, A.A. Nerzhesyan, A.M. Tveslik, “*Bosonization and Strongly Correlated Systems*” , Cambridge Univ. Press, 1998
- [5] D. Senechal, “An introduction to Bosonization”, preprint cond-mat/9908262
- [6] A. Yacoby et al., “Nonuniversal conductance quantization in quantum wires”, Phys. Rev. Lett. **77**, 4612 (1996).
- [7] O. Auslaender, A. Yacoby, R. de Picciotto, K. W. Baldwin, L. N. Pfeiffer, and K. W. West, “Tunneling Spectroscopy of the Elementary Excitations in a One-Dimensional Wire”, Science **295**, 825-828 (2002).
- [8] H. Ishii *et al.*, “Direct observation of Tomonaga-Luttinger-liquid state in carbon nanotubes at low temperatures”, Nature (London) **426**, 540 (2003).

- [9] M. Bockrath *et al.*, “Luttinger-liquid behaviour in carbon nanotubes”, *Nature (London)* **397**, 598 (1999).
- [10] J. Lee, S. Eggert, H. Kim, S.-J. Kahng, H. Shinoara, and Y. Kuk , “Real Space Imaging of One-Dimensional Standing Waves: Direct Evidence for a Luttinger Liquid”, *Phys. Rev. Lett.* **93**, 166403 (2004).
- [11] R. Egger and A.O. Gogolin, “Effective low-energy theory for correlated carbon nanotubes”, *Phys. Rev. Lett.* **79**, 5082 (1997).
- [12] C. Kane, L. Balents, M.P.A. Fisher, “Coulomb interactions and mesoscopic effects in carbon nanotubes”, *Phys. Rev. Lett* **79**, 5086 (1997).
- [13] S. Eggert, “Scanning tunneling microscopy of a Luttinger liquid”, *Phys. Rev. Lett.* **84**, 4413 (2000)
- [14] P. Segovia, D. Purdie, M. Hengsberger and Y. Baer, ”Observation of spin and charge collective modes in one-dimensional metallic chains”, *Nature* **402**, 504 (1999).
- [15] A.E. Mattsson, S. Eggert, and H. Johannesson, “Properties of a Luttinger Liquid with Boundaries at Finite Temperature and Size”, *Phys. Rev. B* **56**, 15615 (1997)
- [16] H.J. Schulz, “Correlation exponents and the metal-insulator transition in the one-dimensional Hubbard model”, *Phys. Rev. Lett.* **64**, 2831 (1990).
- [17] S. Lukyanov. “Low energy effective Hamiltonian for the XXZ spin chain”, *Nucl. Phys.* **B522**, 533 (1998).
- [18] K. Schönhammer and V. Meden, “Spectral sum rules for the Tomonaga-Luttinger model”, *Phys. Rev. B* **48**, 11390-11393 (1993)
- [19] I. Affleck, “Exact correlation amplitude for the Heisenberg antiferromagnetic chain”, *J. Phys. A: Math. Gen.* **31**, 4573 (1998)